# Optimization of a Needle Trap Device

by

Weiqiang Zhan

A thesis

presented to the University of Waterloo

in fulfillment of the

thesis requirement for the degree of

Master of Science

in

Chemistry

Waterloo, Ontario, Canada, 2011

## Author’s Declaration

I hereby declare that I am the sole author of this thesis. This is a true copy of the thesis, including any required final revisions, as accepted by my examiners.

I understand that my thesis may be made electronically available to the public.

## Abstract

Various needle trap devices (NTDs) with different designs for different applications have been developed during the past decade. A theoretical model on the fundamentals of the NTD was recently proposed, which employed the theory of frontal (gas-solid) chromatography to describe the sampling process, where a gaseous sample was continuously introduced into the sorbent bed. In this investigation, different types of sorbent particles with different dimensions were packed into the needle as adsorbents. The effect of particle dimension, which would affect the packing density and consequently the capacity, the extraction efficiency, and desorption efficiency of the NTD were experimentally investigated and the proposed theory was validated. The results demonstrated that NTDs packed with small particles possess higher extraction capacity and efficiency but much higher resistance to flow as well. The higher resistance did not necessarily result in poor desorption efficiency, because desorption efficiency was affected by both the sorbent bed structure and the desorption gas flow. The relationships observed among those physical parameters provide valuable guidance on how to design an NTD with high performance potential for future applications.

For particulate sampling, it was found that NTDs packed with different particles presented high collection efficiency of the particulates being investigated, and the collection efficiency was dominated by the pore size and distribution of the sorbent bed packed inside the needle. Collection efficiency also increased with increase in solidity of the sorbent bed; the increase in humidity of the aerosol sample; and the decrease of sampling rate. The results also provide valuable guidance on the optimisation of needle trap for particulate collection.

## Acknowledgements

I would like to take this opportunity to express my appreciation to all who have supported and assisted me in the completion of my project. First of all, I would like to thank my supervisor, Dr. Janusz Pawliszyn, for offering me such a great opportunity to work on this interesting and challenging project, and for his clear guidance and patient instructions throughout my research work. He was always approachable and helpful when I was in need. Second, I would like to thank my advisory committee members, Dr. Tadeusz Gorecki and Dr. Mario Gauthier, for their valuable advice during my work and critical evaluation of my research. I would like to thank Dr. Gauthier for providing me a chance to audit his polymer courses, which were helpful for my project. I would also like to thank Dr. Gorecki for offering me the use of the analytical balance in his lab, which made my work easier.

I would also like to take this opportunity to express my appreciation to my colleagues for their excellent help during my work period. First, I would like thank Jamie Warren who is actually an excellent “baby sitter”, and who explained and demonstrated many skills required for my work at the very beginning of my project, and who provided vital help when I was in need. I would like to thank Dr. Heather Lord and Dr. Gangfeng Ouyang for their valuable advice throughout my work and their important input to my thesis. I would also like to thank Ruifen Jiang and Dr. Wen-Hsi Cheng for their help and friendship. I would also like to thank all of my other colleagues for the selfless sharing of their knowledge and life experience, which made the research easier and life more interesting, particularly Jong Leu, Paul Togunde, and Yanwei Zhan.

I would also like to thank my colleagues—German Augusto Gomez Rios, Nathaly Reyes Garces, Yanwei Zhan, Ruifen Jiang and Wen-His Cheng for using their initiatives to proofread the draft of the thesis to make it clear and understandable. I would also like to thank Leslie Macumber and James Mackness for their English editing services. I would say the thesis is the outcome of a group of people instead of my own efforts.

I would also like to thank the Natural Sciences and Engineering Research Council of Canada (NSERC) and PAS Technologies Inc. for their financial support.

Finally, I would like to thank my family and friends for their understanding and support while I pursued a master's degree. I would also like to express my special appreciation for their company in my life outside the lab, especially my girlfriend, Cai.

## Dedication

I dedicate this thesis to my beloved parents and my future wife for their love, understanding and support.

# Table of Contents

## List of Figures

## List of Tables

## List of Abbreviations and Symbols

α…….....Packing density of the sorbent bed

*A*…….…...……...Cross-sectional area of the needle

BTEX……Benzene, toluene, ethylbenzene, and *o*-xylene

BTV……...……..Breakthrough volume

CAR……...Carboxen 1000

$C_0$…….....Concentration of the analyte in the sample

CE……..Capillary electrophoresis

$C_s$……...…….....Concentration of the analyte at the surface of the sorbent

*D*……Apparent diffusion constant

$D_0$……..Diffusion coefficient

$d_p$…….....Diameter of the sorbent particle

$d_s$ ……...Sample particle size

DVB…….....Polydivinylbenzene

$\epsilon$……...…….....Single sorbent collection efficiency

E……...Collection efficiency

GC…….....Gas chromatography

$K_{es}$…… Distribution constant of the analytes between extraction phase and sample matrix

$k_p$ ……Permeability of the sorbent bed

*L*……Length of the packed sorbent bed

LC…….Liquid chromatography

LODs……...Limits of detection

LPME…….……Liquid phase microextraction

MEPS……...Microextraction in a packed syringe

*n*……..……..Theoretical plate number

$N_{in}$…….....Number of particles entering the filter

$N_{out}$ ……..……...……Number of particles leaving the filter

NTDs……..Needle trap devices

Δ*p*……..Hydrostatic pressure drop, the pressure difference between the sorbent ends

PAHs……...Polycyclic aromatic hydrocarbons

PDMS……..Polydimethylsiloxane

*Q*……Volume flow rate

*Re* …….....Reynolds number

$S_e$…….……...Surface area of the sorbent packed inside a needle

SPME……Solid phase microextraction

SPE…….Solid phase extraction

ST……...Sorbent trap

*T*. …….....Tortuosity of the sorbent bed

*t*……...Sampling time

$t_e$……Equilibration time

Tenax……...Tenax GC or Tenax TA

TEX……Toluene, ethylbenzene, and *o*-xylene

TWA…….Time weighted average

*u*……...Linear gas velocity

$V_0$ …….....Sample volume

$V_b$ …….……...Breakthrough volume

$V_e$…….……Volume of the extraction phase

$V_t$…….....Breakthrough time

$V_v$…….…….....Void volume of the needle containing the extraction phase

VOCs……Volatile organic compounds

Ø…….....Porosity of the sorbent bed

$\mu$……...Viscosity of the fluid

$\sigma$ ……Root mean square dispersion of the front

# Chapter 1 Introduction

## 1.1 Background introduction

Recently, interest in environmentally friendly, simplified, and miniaturized sample preparation techniques has increased, which has spurred the development of various small, simple, and solvent-free techniques including solid phase microextraction (SPME) [1], liquid phase microextraction (LPME) [2], and sorbent trap (ST) [3]. SPME (shown in Figure 1-1-A) consists of a 22- or 23-gauge stainless steel needle coated with polymeric material as the extraction phase. Extraction is performed by exposing the SPME device to the sample for a predetermined amount of time. LPME (shown in Figure 1-1-B) involves using a liquid drop from the end of the needle tip of a syringe (usually 23- or 24-gauge) as the extraction phase, and employs such device for sampling and sample preparation. Despite the obviously different extraction phases involved during the sampling step, LPME and SPME work on the same principle—equilibrium concept [4]—in that extraction is based on the partition of the analytes between the extraction phase and the sample matrix. The small size of both devices allows convenient instrumental introduction, resulting in a high level of automation using autosampler robots [5]. Another important feature of both techniques is the solvent-free nature of the extraction format and the combination of sampling, sample preparation, and introduction into one single step. The LPME and SPME techniques have already been coupled with gas chromatography (GC), liquid chromatography (LC), and capillary electrophoresis (CE) and then applied to environmental, food, fragrant, forensic, and pharmaceutical

applications [1]. Sensitivity is comparable to traditional large volume extraction methods due to high enrichment of the analytes onto the extraction phase and the introduction of all extracted analytes to instrumental analysis.

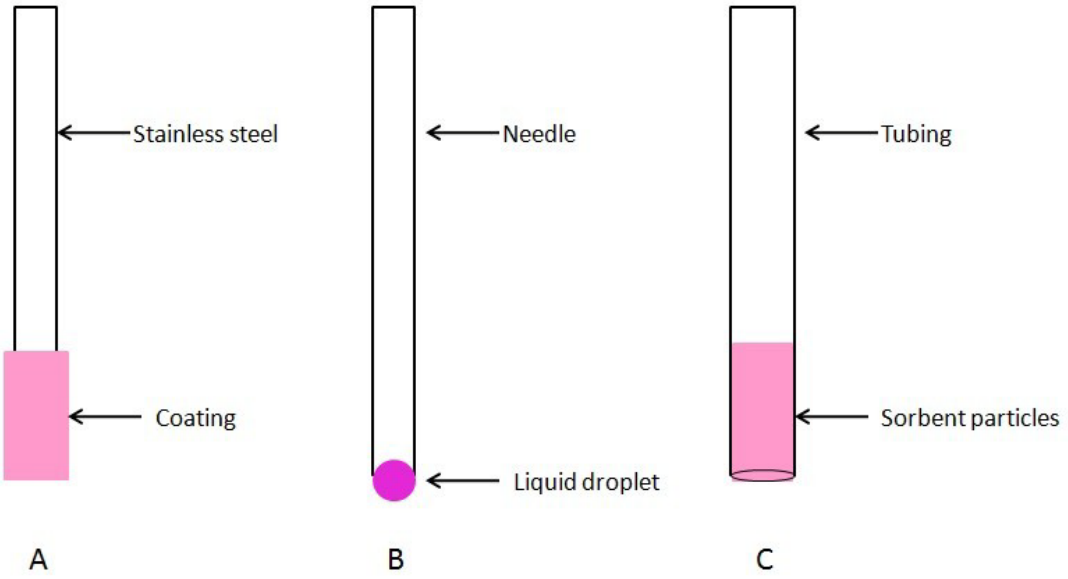


**Figure 1-1 Schematics of: (A) an SPME fibre; (B) an LPME extraction needle; (C) Sorbent trap.**

Instead of exposing the extraction phase directly to the sample matrix, in ST (shown in Figure 1-1-C), a packed sorbent bed (e.g. porous polymer beads) in a tube is used. Extraction and desorption are performed by actively passing an amount of gaseous sample through the tube or by passive diffusion followed by thermal or solvent desorption [2]. The strength of ST, compared with LPME or SPME, is that it is an exhaustive extraction method by nature, which simplifies calibration. The ST technique has been commonly used to determine or monitor volatile organic compounds (VOCs) in air samples, and automated ST systems using thermal desorption methods have been developed for on-site sampling or monitoring [6,7,8,9,10]. However, due to the relatively large amount of sorbent, ranging from 10 mg to several hundred milligrams, the sorbent

trap method suffers from significant thermal resistance combined with an extremely long diffusion path during thermal desorption [11]. Hence, a long desorption time is required and, in some cases, refocusing prior to separation is necessary to achieve better resolution [7]. As a combination of the miniature LPME/SPME and the basic principle of sorbent trap, the needle trap technique has gained increased attention in the past decade. The geometry of NTD is very similar to ST except for the size; ST usually utilizes a 5 cm tube with a diameter of 5 mm or 1 cm packed with 0.2-0.3 mm particles, while an NTD employs a 22- or 23-gauge needle packed with 0.1-0.2 mm particles. Compared with ST, the miniaturized NTD facilitates laboratory automation and on-site sampling compatibility with convenient coupling to analytical instrumentation [5]. NTD also simplifies the calibration and allows particle trapping, which results in total concentration information compared with free concentration data provided by LPME or SPME [5]. Thus, the introduction of NTD is a great supplement for microextraction techniques and a great improvement to ST.

## 1.2 Evolution and method development of NTD

### 1.2.1 Evolution of NTD

The needle trap methodology is not new. Early in the 1970s, Raschdorf reported the use of a syringe needle packed with Tenax for trapping fragrant compounds in the air [12]. More recently in 1996, a similar approach was developed for the preconcentration of gaseous trace organic compounds in natural and industrial air samples and in human breath using charcoal and silica gel sorbents [13]. The approach was found to be rapid and sensitive with detection limits approaching a few ppb. The major limitation of these

earlier methods was the requirement to modify the standard inlet systems due to the large size of the needle, which eliminated their advantage over well-accepted sorbent traps [5].

Needle trap became more practical when needles with smaller diameters were used, which fit conveniently into common GC injectors without modification of the inlet [5]. Early in 2001, an NTD consisting of a 40 mm long 23-gauge needle (O.D. 0.53 mm) and 5 mm quartz wool packing (shown in Figure 1-2-A) was used in Pawliszyn's group to trap particulate matter in different matrices [14]. Sampling was performed by drawing various volumes of air sample (from 0.1 to 5 mL) through the needle, followed by direct insertion of the needle into the GC injection port and the injection of 10 µL clean air into the injector, which aided the introduction of the desorbed analytes to the column. Later in 2005, two NTDs with new designs were introduced and compared by the same group, which are shown in Figure 1-2-B and Figure 1-2-C [15]. Figure 1-2-B shows the NTD with a small side hole in its conical tip in which sorbents were packed segmentally from the tip with polydimethylsiloxane (PDMS) particles, polydivinylbenzene (DVB) particles, and Carboxen 1000 (CAR) particles with thicknesses of 3 mm, 2 mm, and 2 mm, respectively. Quartz wool was packed between the tip of the needle and the side hole. Extraction was performed similar to that of the NTD design in Figure 1-2-A in which the air sample was directly withdrawn through the sorbent bed by a syringe. In regard to desorption, a new carrier gas line system was designed where carrier gas was connected to the needle during the desorption via a valve and re-diverted to the liner when the desorption was done, as shown in Figure 1-3-A. Figure 1-2-C shows another design of the NTD, which has a blunt tip and a side hole positioned 3 cm from the tip, in which 1 cm CAR was packed near the tip of the needle. The side hole was sealed by a septum

during sampling and kept open during desorption. Desorption was performed by directly injecting the NTD into the GC injector equipped with a specific narrow-neck liner, as shown in Figure 1-3-B. The blunt tip of the needle sealed the narrow neck of the liner, forcing the carrier gas to go through the side hole and pass through the sorbent bed to assist with the delivery of the desorbed analytes. It was found that the desorption efficiency of the side hole NTD design was comparable to the conical tip NTD design with the diverted carrier gas system. However, it should be noted that a side hole NTD design coupled with a narrow neck liner was simpler and more convenient since the diversion of carrier gas was not required with this approach. An NTD without a side hole was also tested by Pawliszyn's group [16] but this approach is only applicable for very volatile compounds such as when BTEX is trapped on weak or medium adsorbents without showing severe carryover during desorption. Most recently, the blunt tip of the side hole needle (Figure 1-2-D-b) was modified to have a conical tip (Figure 1-2-D-c) and later still an extended tip (Figure 1-2-D-d) to get better desorption efficiency with a better seal of the needle tip and the narrow neck of the liner [17].

Almost at the same time, Berezkin and co-workers introduced Tenax GC-packed hypodermic needles (0.5 mm I.D. and 0.5 mm O.D.) (Figure 1-4-A) and a tubular cylindrical microconcentrator (Figure 1-4 B), using a 1 mm I.D. and 100-120 mm tube stem with an integrated needle as its end for convenient sample introduction to an analytical instrument. The cylindrical microconcentrator used an external desorption system to facilitate desorption from the large cartridge and it has a similar construction to two high- capacity commercial systems: the CTC ITEX [18] for gaseous and aqueous

headspace samples and the SGE microextraction in packed syringe (MEPS) [19] for liquid samples.

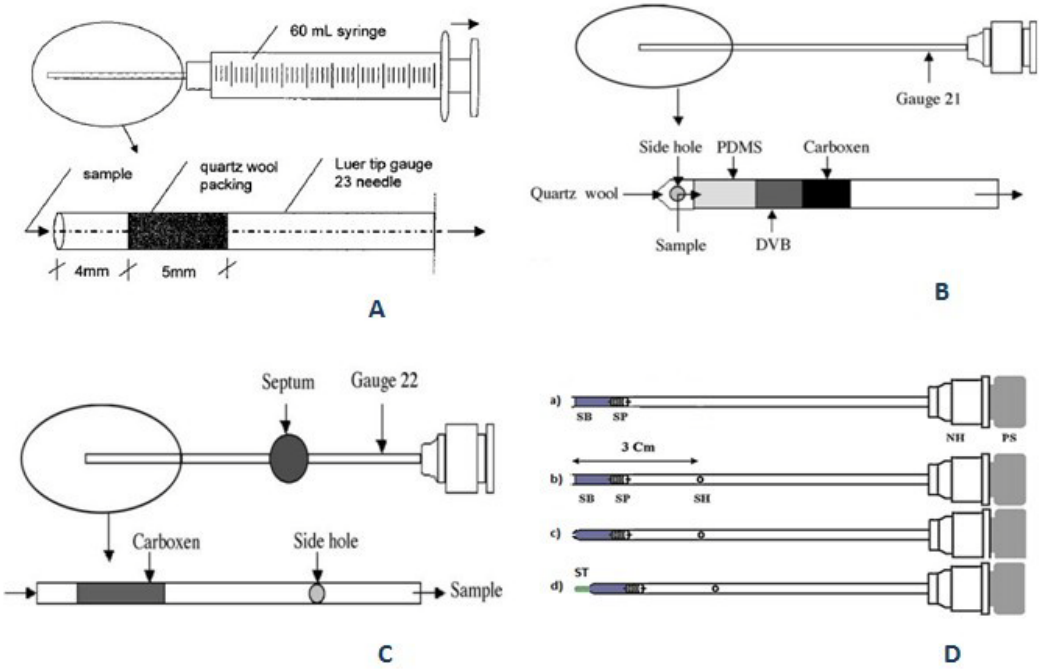


**Figure 1-2 Schematic illustration of the evolution of NTD designs in Pawliszyn's group [14,15,16,17]: (A) a glass wool packed needle; (B) multi-sorbent beds needle; (C) a side hole needle; (D-a) a blunt tip non-side hole needle; (D-b) a blunt tip needle with a side hole; (D-c) a conical tip needle with a side hole; (D-d) an extended tip needle with a side hole**

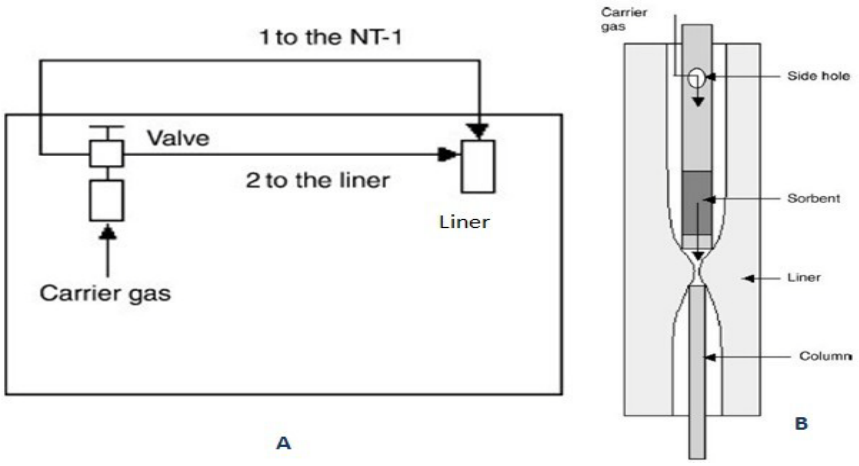


**Figure 1-3 Schematic illustration of A: Carrier gas diverting line; B: NTD inside the narrow neck liner during desorption [15]**

A little later, Jinno introduced needle extraction devices (NeedlEx), which have very similar geometry to the NTDs developed by Pawliszyn (Figure 1-3-B), packed with co-polymer particles (Figure 1-4-C) and polymer-coated fibres (Figure1-4-D) for the determination of VOCs [20], volatile aldehydes [21], breath acetone [22], bisphenol A [23], aromatic compounds [24], and nicotine [25] in either gaseous or aqueous samples. The approaches using these devices were demonstrated to be simple, fast, and convenient.

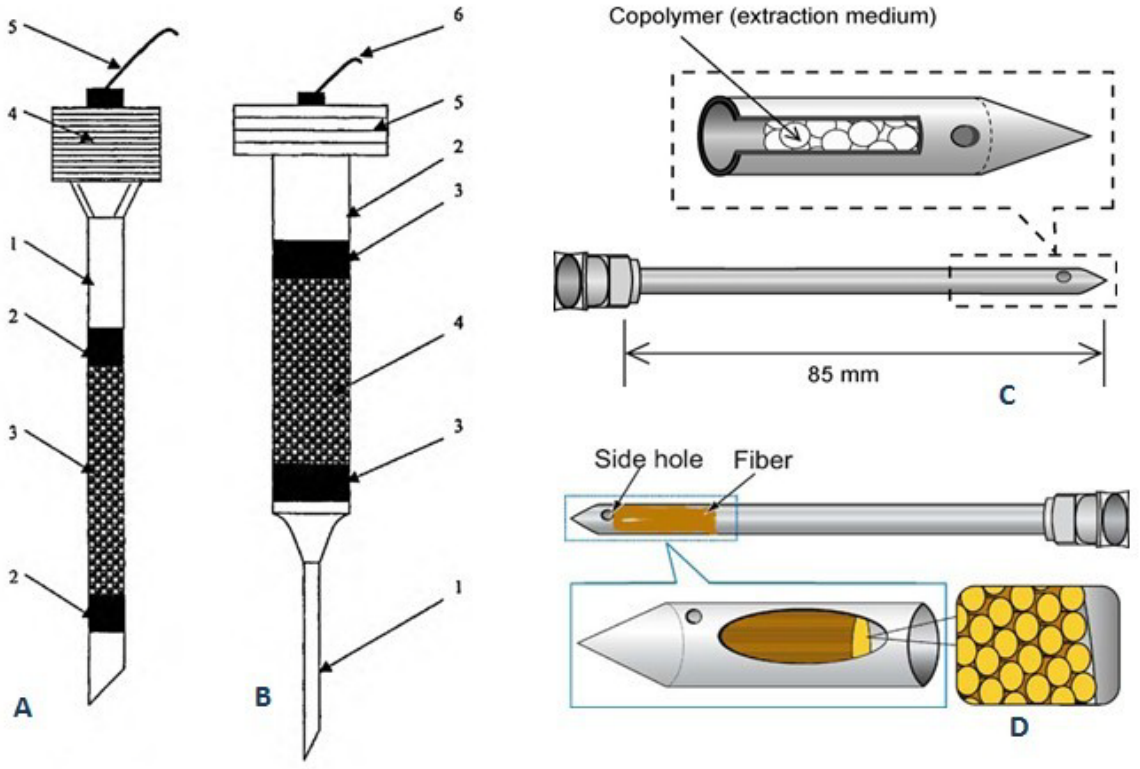


**Figure 1-4 Schematic illustration of (A) Needle microconcentrator: 1-needle stem; 2 plugs, limiting the sorbent layer; 3-sorbent layer; 4-holder; and 5-capillary line for carrier gas. (B) Cylindrical microconcentrator: 1-needle stem; 2-tube stem; 3-plugs, limiting the sorbent layer; 4-sorbent layer; 5-holder; and 6-capillary line for carrier gas. (C) Copolymer particles packed needle. D: Polymer coated fibre packed needle [18,19].**

### 1.2.2 Method development

#### *1.2.2.1 Selection of adsorbent*

Choosing a suitable adsorbent material as the extraction sorbent is a priority for ensuring effective extraction and desorption. The following criteria should be taken into consideration in the selection of a trapping sorbent: strength of interactions between the sorbent and the analytes, which affect both the sorption and release of the analytes from the trapping sorbent; stability; cost; and ease of use. An ideal sorbent should have enough capacity and good affinity towards the target compounds, good physical strength, good thermal stability, and ease of release of the analytes from the adsorbent. The performance characteristics information of the sorbents can be mirrored from the experience with their use in solid phase extraction (SPE) or ST, since method transfer from SPE and ST to needle trap is straightforward. A detailed comparison of adsorbents with different strengths was listed in Ras's review [3], which may serve as a reference for choosing the appropriate adsorbent.

Early applications of NTDs utilized conventional polymer particles, including DVB, CAR, and Tenax, to extract VOCs from gaseous samples [13,15,24,26] or the headspace of aqueous samples [27,28,29]. Those adsorbents performed satisfactorily under those experimental conditions for the analytes investigated. For on-site and in vivo sampling, there was a tendency to immobilize sorbents with different strength to focus on a wider range of analytes. Different types of sorbents were packed in order of weak, medium, and strong, starting from the front needle opening, and the sample was drawn through from weak to strong during sampling. One example can be found in Sanchez's work [30] when discreet sorption beds containing CAR, carbopack X, carbopack B, and

carbopack Y were immobilized inside a needle to quantitatively determine the concentration of 25 organic compounds from 0.8-L breath samples with limits of detection (LODs) in the 1-5 ppb range. Another example can be found in a recent investigation [ 31 ] where the authors utilized multi-bed NTDs packed with CAR, Carbopack X, and Tenax particles for on-site sampling and preconcentration of volatile breath biomarkers with LODs ranging from sub ppt to several ppt and linear correlation coefficients greater than 0.98.

In addition to conventional adsorbents, more polar ones have been proposed and introduced. The group of Jinno introduced the use of newly synthesized particles, consisting of a copolymer of methacrylic acid and ethylene glycol dimethacrylate, as an extraction medium for the concentration of gaseous organic compounds [20]. The results clearly demonstrated the excellent performance for specific organic compounds and suggested future possible applications in working environments. Such material has been used in a commercial needle extraction device (NeedlEx, provided by Shinwa) as the extraction medium for preconcentration of very polar compounds such as formic and acetic acid [32].

Around the same time, the same group also introduced the fibre-in-needle concept and subsequently developed devices (refer to Figure 1-4-D) with a range of polarity characteristics for applications in GC and LC [21,24,25]. The technique was based on coating appropriate polymer material on fibre filaments prior to packing the filaments into a needle. The primary application was to preconcentrate organic compounds in water by directly withdrawing aqueous samples through the fibre bed. A comprehensive

summary on the applications of the fibre packed needle can be found in a recent review [33].

Some novel materials based on carbon nanotubes were also investigated recently [34,35]. Bagheri [34] studied the use of carbon nanotube-sol-gel-based sorbents for the microextraction of polycyclic aromatic hydrocarbons from aquatic media and Sae-Khow [35] investigated the implementation of nanomaterials in the needle of a syringe for the determination of nitrophenol, dichloroaniline, and naphthalene. Both methods exhibited good linearity, good repeatability and low LODs, indicating the potential application of the novel nano material in NTD.

#### *1.2.2.2 Sampling mode*

One distinguished advantage of an NTD compared with SPME or LPME is that the NTD is able to act as an active sampler via connecting with a pump or gas-tight syringe. To finish an active sampling, a certain volume of gas or liquid sample is drawn through the needle by a pump or syringe and the target analytes are retained on the sorbent. Active sampling allows a higher sampling rate in comparison with passive sampling and it also allows the use of multi-sorbent beds.

NTD is also able to effectively perform time-weighted-average (TWA) diffusive sampling. Using this sampling mode, NTD packed with the sorbent at a defined distance from the needle opening is exposed to the sample matrix for a certain period of time. Analytes enrich onto the sorbent due to the diffusion of the analytes through the needle from the immediate surroundings to the sorbent bed. Since the adsorbent has a strong affinity for the analytes, a concentration gradient can be established to favour diffusion of

the analytes from the sample to the adsorbent. Thus, the retained amount can be calculated based on the integral of the analyte concentration over time and space.

### *1.2.2.3 Desorption method*

#### *1.2.2.3.1 Desorption method overview*

Achieving efficient desorption with NTDs has been the focus of many researchers. To date, both thermal desorption and solvent desorption methods have been successfully applied to NTDs to release the analytes from the sorbent bed prior to their introduction into a column. In regard to thermal desorption, several approaches have been investigated to date, including external gas assisted desorption, having carrier gas flow through the needle directly, thermal expansion, and heated water vapour desorption.

#### *1.2.2.3.2 External gas assisted desorption*

Earlier applications of NTDs utilized external gases, including air, nitrogen, and helium, to aid desorption. In this simple technique, a certain amount of clean gas is drawn into the syringe and expelled after injection of the needle into a GC injection port to aid the delivery of the desorbed analytes and consequently resulted in more efficient desorption. The initial application of this technique utilized 10 µL of air to aid with the desorption of diesel exhaust compounds from the NTD consisting of a 5 mm quartz wool bed packed into a 23-gauge needle [14]. This simple method was later applied by Ueta [22], Saito [20], and Lou [33] for the analysis of breath acetone, VOCs, and acetic acids, respectively. No carryover was reported in any of the above studies for the analytes investigated.

#### *1.2.2.3.3 Carrier gas flow desorption*

Numerous authors have recognized that superior desorption performance may be obtained by using carrier gas passed through the sorbent bed during thermal desorption. The major disadvantages of using a syringe filled with either air or inert gas includes the introduction of oxygen to the sorbent, which might shorten the sorbent life, and a potentially insufficient amount of desorption gas to completely release all analytes [5].

Two approaches to introduce carrier gas into the needle have been described including diverting the carrier gas flow to the needle during the desorption and using a side hole 3 cm from the tip as the introduction port [15]. The first approach (Figure 1-C-A) employed a secondary carrier gas split valve. In separation mode, the carrier gas flowed into the injector and through the column as usual, but during desorption an external gas line from the split valve was connected to the back of the NTD and carrier gas was directed to flow through the needle. After desorption, carrier gas flowed into the injector again by use of an automatic switch. Another approach utilized a needle with a side-hole positioned about 3 cm back from the tip of the needle, with sorbent packed between the side hole and the tip. A narrow neck liner (Figure 1-3-B) was required for this approach. When the needle trap was injected down to the narrow neck point of the liner, the tip of the needle was sealed against the narrow neck. Carrier gas flow was then automatically directed into the side hole and passed through the sorbent before entering the column. No carryover effect was observed by this approach. The latter approach was thought to be more convenient and simpler than the first approach since no modification of the carrier gas line was required. Further efforts were focused on modifying the tip of the side hole needle and the narrow neck liner to get better sealing using the latter

approach [17]. The side hole needles with blunt tip (Figure 1-2-D-b), conical tip (Figure 1-2-D-c), and extended tip (Figure 1-2-D-d) were compared, and it was found that the best seal was obtained by the side hole needle with an extended tip, which was later commercialized by SGE Analytical Science.

#### *1.2.2.3.4 Thermal expansion desorption*

In contrast with providing a desorptive flow through the needle during desorption, the thermal expansion desorption approach employs the expanded gas flow, which results from the sharp increase in temperature inside the needle when it is injected into a heated GC injector, to assist with desorption. Simply inserting an NTD into a hot GC injector and removing it after a desired desorption time are the only steps for completing analytes desorption. This method was employed by Eom and Pawlisyzn [16] for thermal desorption of benzene, toluene, ethylbenzene, and *o*-xylene (BTEX), and an alkane mixture (C6-C15) from a packed DVB sorbent bed. A carryover of up to 1.1% was observed for BTEX compounds, indicating that this simple desorption method can be effectively applied to the analysis of volatile compounds with a weaker sorbent.

Thermal expansion desorption is the simplest sample desorption method, in which no side hole or external desorptive flow is required, but this technique has not been widely applied in needle trap, likely due to the limitation of desorption carryover for less volatile compounds or strong adsorbents, and high dependence on the analytes and sorbent type [5].

#### *1.2.2.3.5 Heated water vapour desorption*

Several authors have observed improved desorption efficiency when a huge amount of water vapour or droplets was present inside the needle during thermal expansion-desorption. Such observation was later demonstrated by Prikryl [36]. In the study, the needle microconcentrator was packed with segmented layers of DVB and alumina, which were used to enrich VOCs and water vapour separately. After the enrichment of BTEX from water by dynamic headspace sampling, the alumina layer was saturated with water and the device was then inserted into a GC injector for thermal desorption. The water on the alumina layer vaporized quickly due to the hot injector temperature, which flushed the BTEX compounds into the separation column. A clean and sharp BTEX chromatogram was achieved, but the use of water might be problematic. The massive water injection might produce a long tailing water peak with high noise. In addition, the injection of water can shorten column lifetime and cause possible interferences with detectors [5].

#### *1.2.2.3.5 Solvent flushing desorption*

The solvent desorption method has also been applied for the transfer of the analytes from the sorbent bed to the column. This approach is performed by filling a gas-tight syringe with solvent and air and then connecting it to the needle, then introducing the needle into the hot GC injector. Solvent and air then flush through the sorbent bed to desorb the analytes [21,23, 25,33]. The adoption of the solvent desorption method in needle trap enables the analyses of semi-volatile and non-volatile compounds and the coupling of NTD with LC. However, this approach has only been conducted with

filament-packed needles rather than with particle-packed needles. Further investigations need to be done on this subject with particle-packed NTDs.

### 1.2.3 Applications

#### *1.2.3.1 VOCs and some other compounds*

Early applications of NTDs focused mainly on the determination of VOCs in gaseous and aqueous matrices. In 2003, Berezkin et al. [37] packed hypodermic needles (0.5 mm I.D. and 0.8 mm O.D.) with Tenax as a microconcentration device to extract benzene and toluene from tobacco smoke. It was found that the experimental results were in good accordance with the previous study. Subsequently, with a similar NTD, Kubince and co-workers developed a needle-based direct water extraction system with Porapack Q as a sorbent material and wet alumina as a source of desorptive water vapour flow to analyze BTEX in aqueous samples [27]. The experimental results showed that the detection limit of the needle trap device was comparable to those purge and trap techniques. Additional work conducted by Berezkin and co-workers [36] proved that such extraction device was comparable to SPME in simplicity and flexibility but with much higher sorbent capacity. Following the success of a quartz wool-packed needle for extracting particulates from diesel exhaust, a dose of aerosolized asthma drug, and insect repellent spray in 2001 [14], Pawliszyn and co-workers proposed and demonstrated in 2005 the use of a multi-adsorbent trap for the extraction of a wide range of volatile compounds and the use of a side hole above the sorbent bed to introduce the carrier gas into the needle to help desorption [15]. Later, the side hole needles packed with DVB or CAR particles were used for sampling BTEX from air with detection limits below 0.1 ng/mL [26], followed by the establishment of a needle trap-based syringe pump assisted

dynamic headspace sampling system for the analysis of BTEX from aqueous samples with LODs below 1 ng/mL [28]. Around the same time, NTDs packed with co-polymer particles were developed by Jinno and co-workers to determine gaseous organic compounds [20]. The results clearly demonstrated excellent extraction performance of such devices for specific organic compounds. Later, the same group introduced and applied the fibre packed needle for the analysis of more polar or less volatile compounds, including smoking-related compounds in hair and air samples [25], breath acetone [22], and bisphenol A in water [23]. From these applications, NTD was demonstrated to be a robust, fast, and easily automated method with high sensitivity.

#### *1.2.3.2 Particulates*

The most appealing characteristic of NTD may be that it can act both as a filter and the extraction sorbent and, therefore, it is able to extract both particle bound chemicals and free molecules simultaneously. This characteristic has already been demonstrated by Koziel [14] and Niri [38].

Koziel and co-workers [14] packed quartz wool with a packing length of 5 mm inside a 23-gauge needle, to determine the total concentration of polycyclic aromatic hydrocarbons (PAHs) in diesel exhaust, and triamcinolone acetonide in aerosolized asthma. A 7 μm SPME fibre was used to simultaneously determine the free concentration of the analytes. The results showed that both NTD and SPME yielded similar qualitative results with respect to major classes of detected analytes and NTD could be used as a fast screening tool for analysis of airborne particulates in exhaust samples. Another application of the NTD for the determination of the total concentration of allethrin in mosquito coil smoke was later described by Niri and co-workers [38]. Employing SPME

and NTD simultaneously under the same sampling conditions, the extracted amount of allethrin from the NTD was higher than from the SPME fibre.

When an aerosol or particulate sample passes through the sorbent bed, free molecules are retained onto the surface of the sorbent bed while particles collide and attach to the surface of the sorbent. There are four basic mechanical collection mechanisms by which a particulate can be deposited onto a sorbent including interception, inertial impaction, diffusion, and gravitational settling. The contribution of each mechanism varies with respect to sorbent particle size as well as collected particulate size. By choosing appropriate sorbent particle size and sampling flow rate, we are able to collect particulates with different ranges of sizes [38].

## 1.3 Theoretical considerations

### 1.3.1 Active sampling

In a needle trap, since the gaseous sample is continuously introduced into the needle, the process of extraction inside the needle can be described as frontal (gas-solid) chromatography. The capacity of the column—the packed needle in this case—is described by the breakthrough volume (BTV) and it is affected by gas pressure, temperature, humidity, flow rate, and sorbent bed geometry [39], and is closely related to the shape of the eluting front which can be described as the integral of a Gaussian peak.

Based on the frontal chromatography assumption, many attempts [40,41,42] have been made to find a mathematical relationship between sampling capacity and chromatography parameters such as the retention volume and the number of theoretical

plate. Among those, the model developed by Lovkvist [42] is the most appropriate for needle trap. In this model, the theoretical plate number is expressed as:

$$n = \frac{uL}{2D} \qquad (1)$$

Where $L$ is the length of the packed sorbent bed, $D$ is the apparent diffusion constant which is intended to include all mechanisms of dispersion, $u$ is the linear gas velocity.

The apparent diffusion constant could be defined as

$$D = \frac{1}{T^2} D_0 + T d_p u \qquad (2)$$

Where $T$ is the tortuosity of the sorbent bed, $D_0$ is the diffusion coefficient, and $d_p$ is the diameter of the sorbent particle.

Ignoring the gas compressibility and assuming that the flow rate is constant, the linear flow rate ($u$) of the gas sample through the needle can be intuitively described by:

$$u = \frac{Q}{A\emptyset} \qquad (3)$$

Where $Q$ is the volume flow rate in the needle, $A$ is the cross-sectional area of the needle, $\emptyset$ is the porosity of the sorbent bed.

The volume flow rate can be defined by [43]

$$Q = \left(k_p A/\mu\right)(\Delta p/L) \qquad (4)$$

Where $\Delta p$ is the hydrostatic pressure drop, and $\mu$ is the viscosity of the fluid, $k_p$ is the permeability of the sorbent bed, which is related to the surface average sphere diameter of the particle, $d_p$, and the porosity of the sorbent bed, $\emptyset$.

The time required to complete sampling a given volume $Q_0$ of the sample then can be calculated by:

$$t_s = \frac{Q_0}{Q} \qquad (5)$$

In frontal chromatography arrangements, the concentration profile along the *x*-axis, of the needle containing the extraction phase, as a function of time *t*, can be described by adopting and deriving the expression for dispersion of a concentration front [42]:

$$C(x,t) = \frac{1}{2}c_0\left(1 - erf\frac{x-\frac{ut}{L(1+k)}}{\sigma L\sqrt{2}}\right) - \frac{1}{2}c_0 \times \exp(2n) \times (1 - erf\frac{x-\frac{ut}{L(1+k)}+2}{\sigma L\sqrt{2}}) \qquad (6)$$

Where $c_0$ is the concentration of analyte in the sample, *k* is the retention factor defined as:

$$k = K_{es}\frac{V_e}{V_v} \qquad (7)$$

Where $K_{es}$ is the partition constant of the analytes between the extraction phase and the sample matrix, $V_e$ is the volume of the extraction phase, and $V_v$ is the void volume of the needle containing the extraction phase.

$\sigma$ is the root mean square dispersion of the front defined as:

$$\sigma = \sqrt{\frac{L}{n}\frac{ut}{1+k}} = \sqrt{\frac{2Dt}{1+k}} \qquad (8)$$

The difference between Equation (6) and other frontal equations is that it is more applicable when *n* is very small, where *n* is usually small in needle trap due to the short sorbent bed [42].

Figure 1-5 illustrates the normalized concentration profiles produced in the bed during extraction based on Equation (6). Full breakthrough is obtained for the right-most curve, which corresponds to the appropriate volume of the sample matrix for extraction.

The time required to pass this volume through the extraction system corresponds to the equilibration time of the compounds with the bed, and the equilibration time can be assumed as the time required for the center of the front to reach the end of the sorbent:

$$t_e = \frac{L(1+k)}{u} \qquad (9)$$

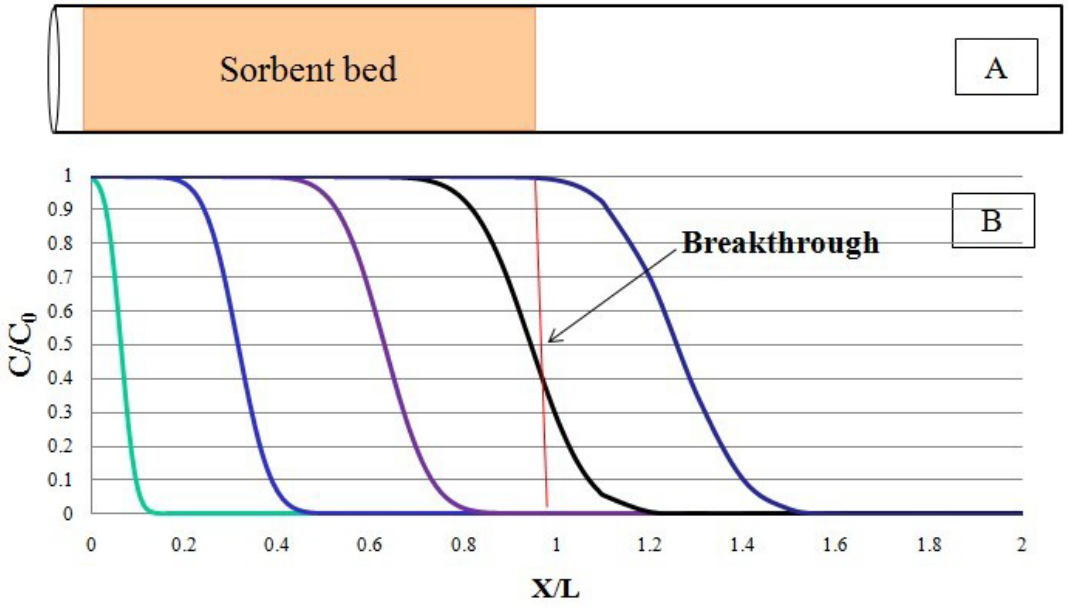


**Figure 1-5 A: Schematic representation of a packed needle; B: Theoretical concentration profiles in the sorbent bed, where C is the concentration of the analyte in the sample, L is the length of the sorbent bed, X is the relative position along L.**

During sampling, before breakthrough, the sorbent bed could be treated as "perfect sink" for analytes. In this case, the mass of a certain analyte loaded in the sorbent bed can be described as the total mass flowing through the beginning of the sorbent bed (when $x = 0$ in Equation (6)):

$$n(t) = Au\emptyset \int_0^t C(0,t)dt = A\emptyset u c_0 t = c_0 V_0 \qquad (10)$$

The breakthrough level then can be defined as the percentage of mass exiting the end of the sorbent bed compared with the initial mass passing through the beginning of the sorbent bed:

$$b = \frac{Au\emptyset \int_0^t C(L,t)dt}{A\emptyset u c_s t} = \frac{\int_0^t C(L,t)dt}{c_s t} \qquad (11)$$

The approximated solution of *b* can be found in Lovkvist's work [42], from which the breakthrough time is obtained by derivation:

$$t_b = \frac{L(1+k)}{u}\left[(1-b)^2 + \frac{a_1}{n} + \frac{a_2}{n^2}\right]^{-1/2} \qquad (12)$$

Where $a_1, a_2$ are complicated functions of *b*, and the values of $a_1$, $a_2$ corresponding to *b* were provided in the work of Lovkvist as well.

We assume breakthrough happens when $b \geq 5\%$. When *b*=5%, $a_1 = 5.360, a_2 = 4.603$. As a result, Equation (12) could be rewritten as:

$$t_b = \frac{L(1+k)}{u}\left[0.903 + \frac{5.360}{n} + \frac{4.603}{n^2}\right]^{-1/2} \qquad (13)$$

Converting the breakthrough from the time scale to the volume scale, we obtain the breakthrough volume in Equation (14) where

$$V_b = A\emptyset L(1+k)\left[0.903 + \frac{5.360}{n} + \frac{4.603}{n^2}\right]^{-1/2} \qquad (14)$$

Comparing Equation (9) and Equation (13), $t_e$ is very close to $t_b$ at high plate number (i.e. $n$>10). Therefore, at high plate numbers, Equation (9) can be used to calculate the breakthrough time as an approximation.

The above gives valuable guidance on how to construct the NTDs for chemical trapping. To get a higher sampling rate and reduce the sampling time, good permeability of a NTD should be maintained; while for obtaining efficient trapping without breakthrough, an efficient packing (dense packing) is preferred. Therefore, the porosity should maintain a certain range. Large particle size would be helpful to decrease the resistance but disadvantageous for increasing the capacity since large particles would decrease the packing density. For obtaining a higher capacity, a longer sorbent bed can be used; however, this would result in an increase in the resistance. As a result, a needle with a relatively larger diameter may be used to increase the capacity without suffering from an increased resistance. Moreover, a stronger adsorbent may be used to increase the capacity when a good desorption efficiency is guaranteed. However, due to limited surface area, the adsorbent is easily saturated at high concentrations long before an equilibrium condition has been achieved, and since the above model was based on a linear distribution isotherm assumption, it is more applicable at sufficiently low concentrations. Nevertheless, it could be quite useful to predict the maximum sampling time or breakthrough volume in on-site sampling since in such places, the concentrations are usually low and a much longer sampling time is required.

### 1.3.2 Particle sampling

The capture of aerosol particles by filtration is the most common method of aerosol sampling and a widely used method for air cleaning. In theory, the NTD is able to act as a filter to trap particulate matter on the sorbent by passing the aerosol sample through the device. The ability of an NTD to collect particles can be similarly characterized by single fibre theory [44], where the NTD efficiency can be estimated by

integrating the single collection efficiencies for the whole sorbent length $L$, composed by the sorbent particles with diameter $d_s$; a simplified equation is expressed below:

$$E = \frac{N_{in} - N_{out}}{N_{in}} = 1 - \exp\left(\frac{-4\alpha L\epsilon}{\pi d_s}\right) \qquad (15)$$

Where $N_{in}$ and $N_{out}$ refer to the number of particles entering and leaving the filter, respectively, $\alpha$ is the solidity of the sorbent bed, and $\epsilon$ is the single sorbent collection efficiency.

To determine the single sorbent collection efficiency, we have to first explain the mechanical trapping mechanisms. There are four mechanical collection mechanisms by which aerosol particles can be trapped by an NTD: interception, inertial impaction, diffusion, and gravitational settling [45]. Interception happens when a particle follows a gas stream that happens to come within one particle radius of the surface of a sorbent particle [45]. The single sorbent efficiency for interception is closely related to the ratio of particle diameter to sorbent diameter, and the packing density [45]. Inertial impaction occurs when a particle, because of its inertia, is unable to adjust quickly enough to the abruptly changed streamlines in the vicinity of a sorbent particle and crosses those streamlines to hit the sorbent particle [45]. Its efficiency is governed by the value of the Stokes number and related to the ratio of particle diameter to sorbent diameter, as well as the packing density [45]. Diffusion is caused by the Brownian motion of small particles, which is sufficient to greatly enhance the probability of their hitting a sorbent particle while traveling past it on a nonintercepting streamline [45]. The efficiency of diffusion is related to the particle size of the sorbent, the linear flow rate, and the diffusion coefficient

of the particle [45]. Gravitational settling is negligible compared with the other three mechanisms [45]. A schematic diagram of those mechanisms is shown in Figure 1-6.

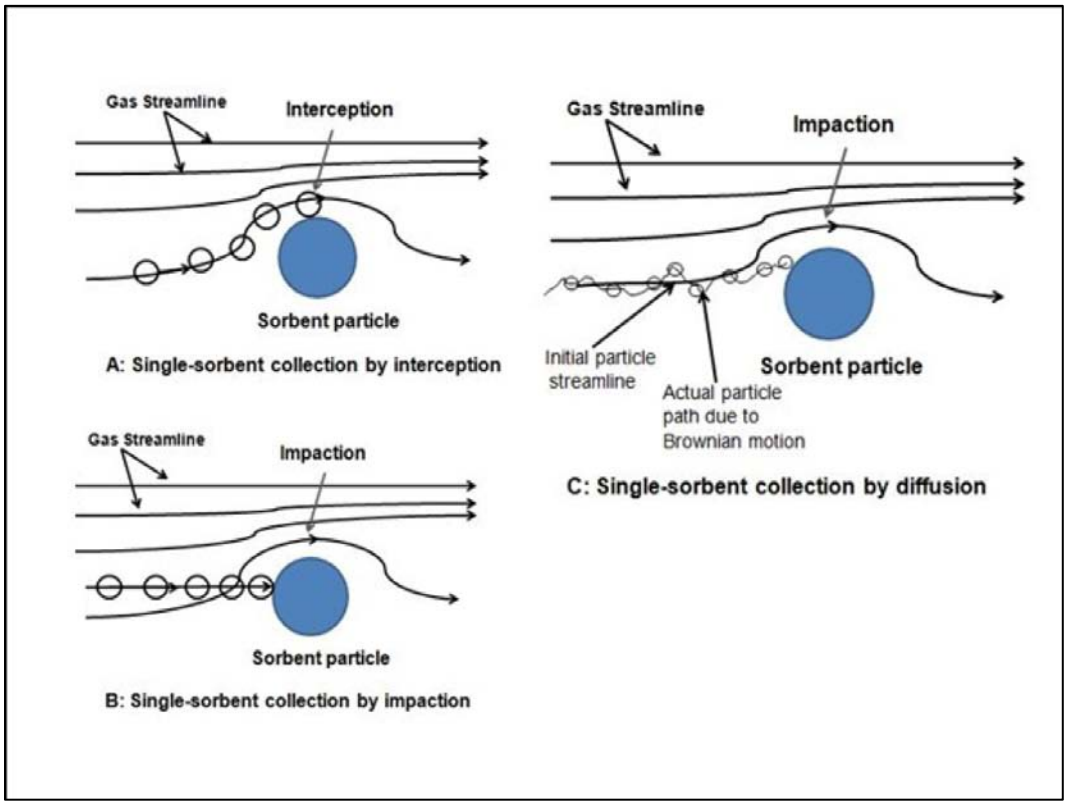


**Figure 1-6 Schematic explanation of interception, impaction, and diffusion [5]**

Mathematical equations for the collection efficiencies of the above mechanisms for traditional fibrous filters have already been investigated, and the total sorbent collection efficiency can be estimated as a sum of the above mechanisms. The total efficiency, as well as each single efficiency, are illustrated in Figure 1-7. In estimating the overall single-sorbent collection efficiency near the size of minimum efficiency, it is necessary to include an interaction term—DR interaction—to account for enhanced collection due to interception of the diffusion particles. As seen from Figure 1-7, for larger particles (typically above 0.5 μm), inertial impaction and interception tend to predominate the

trapping efficiency, while for small particles (typically below 0.2 μm), diffusion is the dominant collection mechanism, and other mechanisms are considered to be negligible [46]. Breakthrough happens for particles from about 0.2 μm to about 0.5 μm. It is reasonable that particles between 0.2 μm and 0.5 μm are too large for diffusion to be effective, and too small for interception and impaction to be effective. Such results are confirmed when the collection efficiencies of NTDs with different packing for a wide range of particulates are illustrated in Figure 1-8.

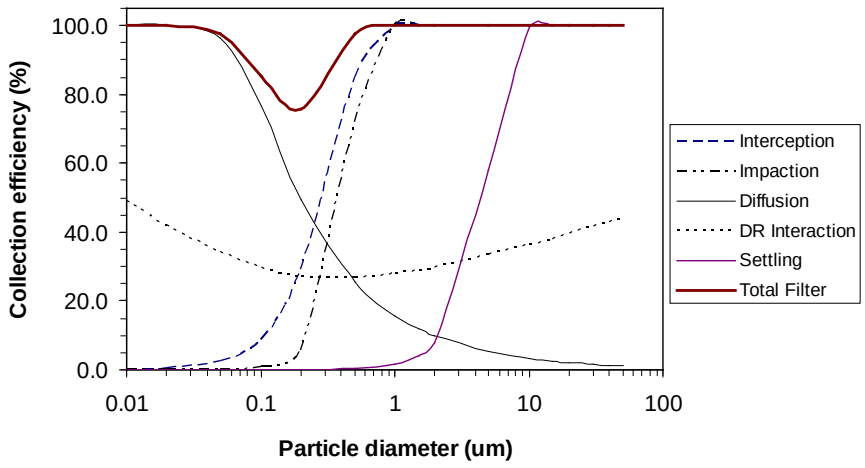


**Figure 1-7 Illustration of collection efficiency for individual single-sorbent mechanisms and total efficiency; $L$=1 mm, $\alpha$=0.05, $d_p$= 2μm and $u$= 10 cm/s [45]**

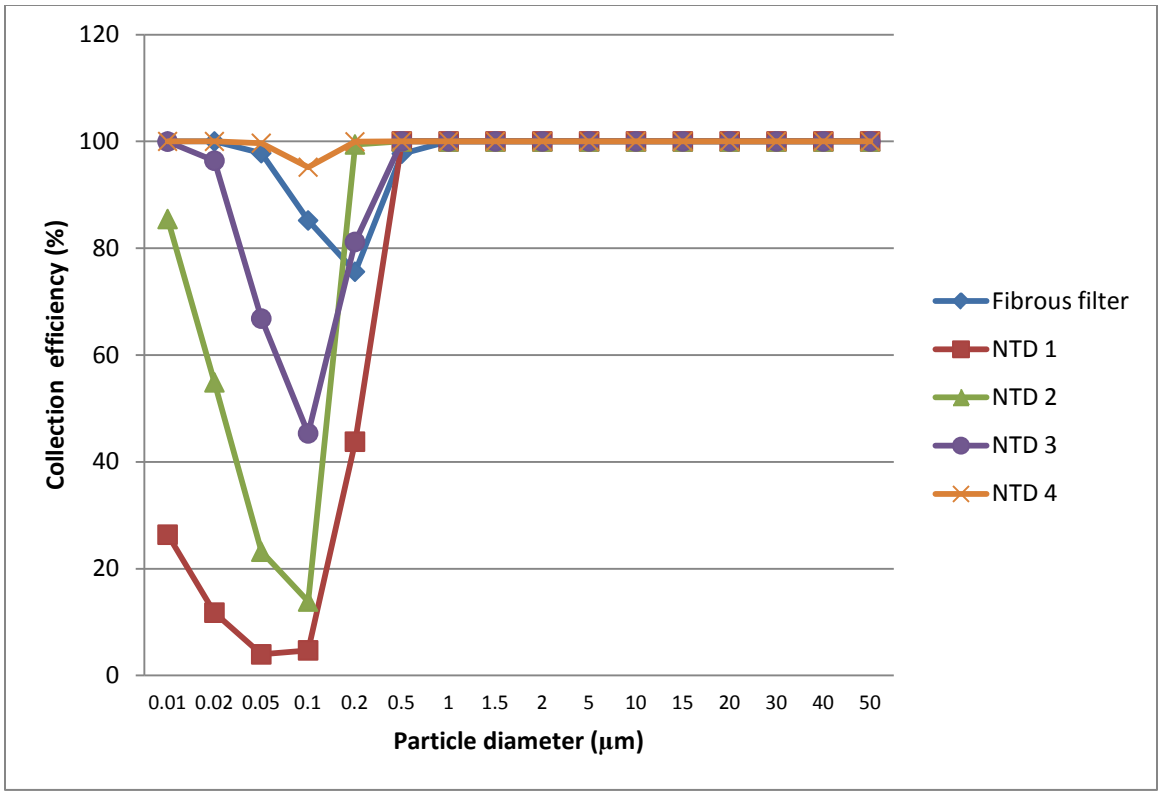


**Figure 1-8 Extraction efficiencies for the fibrous filter and the needle trap devices (fibrous filter: thickness=1 mm, solidity=0.05, sorbent diameter=2 µm and the linear flow rate is 10 cm/s; NTD 1: packed with sorbent particles, the length of sorbent bed= 10 mm, solidity=0.35, sorbent particle diameter=150 µm, and the linear flow rate of sampling is 100 cm/s; NTD 2: packed with sorbent particles, the length of sorbent bed=10 mm, solidity=0.35, sorbent particle diameter=50 µm, and the linear flow rate is 100 cm/s; NTD 3: packed with glass wool, the length of the sorbent bed= 10 mm, solidity=0.10, sorbent particle diameter = 10 µm, and the linear flow rate of sampling is 100 cm/s; NTD 4: packed with thinner glass wool, the length of sorbent bed= 10 mm, solidity =0.10, sorbent particle diameter = 5 µm, and the linear flow rate of sampling is 50 cm/s) [5]**

As shown in Figure 1-8, the conventional NTDs (NTD 1) packed with particles with sizes of about 150 µm are only able to completely trap the particles with a diameter larger than 0.5 µm. Even when the NTDs are packed with smaller sorbent particles, the penetration of the sample particles might decrease but still be significant (NTD 2). It should be noted that for NTDs packed with sorbent particles, all the theoretical

calculations are based on the assumption that the particles packed inside the needle are spherical solid beads without pores inside the particles, and the penetration is mainly caused by the penetration of particles through inter-particle pores. However, in practice, porous particles with irregular shapes are often used as adsorbent inside the needles. The irregular shapes of the particles might increase the packing density and reduce the inter-particle pores and consequently reduce the penetration, while the intra-particle pores might increase the trapping efficiency as well. Therefore, the trapping efficiency of NTDs packed with porous particles may be different from the theoretical calculations, but it is still possible that particles of certain sizes will penetrate the sorbent bed without being trapped. One possible solution to this penetration problem might be packing the needles with glass wool, which has a small sorbent diameter but also a large porosity (see NTD 3 and 4). During the sampling process, the sorbent with a small sorbent diameter would help to decrease penetration significantly, while the large porosity would avoid a considerable increase in the resistance of the sorbent bed. By packing the glass wool, especially silanized glass wool in the front of a needle to trap the particles, while packing other sorbent particles afterwards to extract free molecules, the NTD may be able to trap free molecules and particles simultaneously.

## 1.4 Objective of this project

As discussed from the theory, the capacity of an NTD increases with the increase of the cross-sectional area of the needle, the porosity and the length of the sorbent bed, and the retention factor, as well as the theoretical plate number, while the resistance of an NTD increases with the increase of the length of the sorbent bed, and the decrease of the porosity. Ideally, an NTD should have a large capacity with little resistance in order to

obtain a low detection limit and to increase the sampling rate so as to reduce sampling time. The porosity of the sorbent bed is mainly affected by the dimensions of the particles packed inside the needle. Therefore, the main objective of this project is to validate the theory and investigate the influence of the sorbent particle size on the performance of the NTD before optimization.

The NTD has already been proven able to act as a filter to trap particulates, but the trapping efficiency towards particles of different sizes has not yet been investigated. Another objective of this work is to investigate whether, and under what circumstances, the NTD is able to trap the particles at high efficiency, and also to optimize the NTD performance for particulate trapping.

# Chapter 2 Optimization of packing material and packing method

## 2.1 Introduction

According to Equation (4) (Page 18), the volumetric flow rate of each needle is proportional to the permeability ($k_p$) of the sorbent bed and the cross-sectional area ($A$) of the needle, and inversely proportional to the length of the sorbent bed ($L$). If there is gas flow under a certain pressure passing through the sorbent bed, the actual volumetric flow rate will reflect the resistance of each needle. The higher the flow rate, the lower the resistance will be. Theoretically, a small resistance, reflected by a high flow rate, is helpful for efficient desorption, which means a large permeability of the sorbent bed is usually desired in NTD. The concept of permeability is similar to the conductivity of an electrical wire for electrons; it is a term used to measure the conductivity of the porous sorbent bed with respect to permeation by a Newtonian fluid [43]. Permeability takes into account every factor that might affect the permeation, without discussing the pore structure and size distribution of the sorbent bed, and is mainly related to porosity (∅), pore structure and the holding material on the two ends of the sorbent bed. The permeability of NTD can be determined experimentally using the following transformation of Equation (4), where

$$k_p = Q\mu L/(A\Delta p) \qquad (16)$$

Although a large variety of materials including quartz wool [14], Tenax [37], DVB [16,28,32], and CAR [15, 26] have been used as adsorbents in particle-packed NTDs, only 60/80 mesh has been investigated with respect to the particle size for almost all of the adsorbents. No fundamental discussions regarding the influence of the particle

size or the packing length on the permeability (reflected by the flow rate) are found to date. Furthermore, although several materials including glue, stainless spring wire, and glass wool have been applied to immobilize the sorbent, their influences on the permeability of the needle have not yet been investigated. Therefore, the objective of this part of the work is to investigate the influence of the particle size, the packing length, and the immobilizing material on the permeability of the NTD.

## 2.2 Experimental section

### 2.2.1 Chemicals and materials

CAR particles (surface area: 1200 $m^2/g$) of 60/80 mesh, 80/100 mesh, and 100/120 mesh were purchased from Sigma-Aldrich (Bellefonte, PA, USA). DVB particles (surface area: 582 $m^2/g$) of 60/80 mesh, 80/100 mesh and 100/120 mesh were purchased from Ohio Valley (Marietta, OH, USA). The 3.5 inch long 22-gauge blunt needles (I.D. 0.41 mm, O.D. 0.71 mm) were purchased from Dyna Medical Corporation (London, ON, Canada). Stainless steel wires (O.D. 100 µm) were purchased from Small Parts (Lexington, KY, US). The 5-min epoxy glue was purchased from Henkel Canada (Mississauga, Ontario, Canada). The ADM 1000 flow meter was purchased from Agilent Technologies (Mississauga, ON, Canada). The microbalance (MXA 21) with a resolution of 1 µg was purchased from RADWAG (Radom, Poland).

### 2.2.2 Preparation of NTD

To prepare an NTD, first, the stainless wire was pressed by two steel guides and fixed into the desired position as a spring plug (Step 1 in Figure 2-1). Then, sorbent

particles were aspirated into the needle by a tap-water aspirator and held by the spring plug (Step 2 in Figure 2-1). After packing the desired length of sorbent bed, an extremely small amount of epoxy glue was used to immobilize the sorbent from the opening end (Step 3 in Figure 2-1). During the packing process, the aspirator was kept running until the epoxy glue was cured to avoid the blockage of the NTD by the epoxy glue. The whole process was similar to previous work [15], but the needles were weighed before and after packing to determine the amount of the sorbent inside the needle. All of the sorbent beds in the NTDs were immobilized by glue at the opening ends, unless indicated.

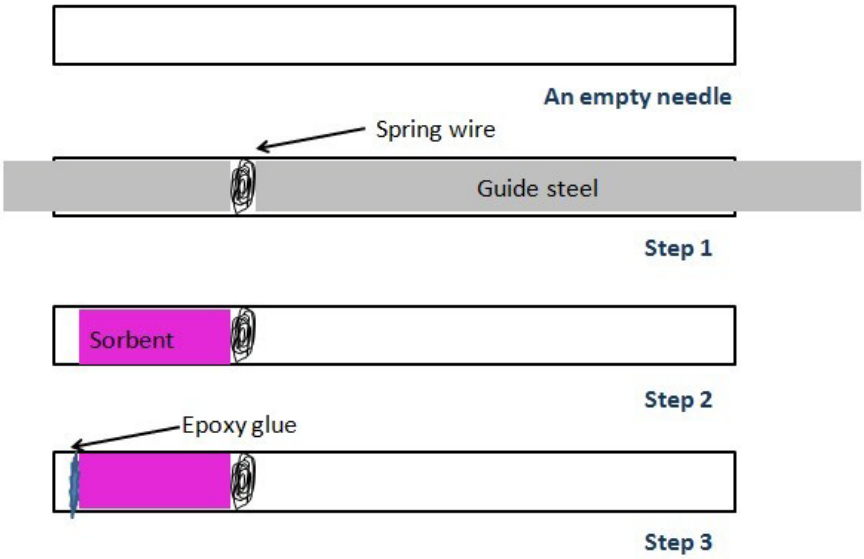


**Figure 2-1 Schematic illustration of the packing procedure**

### 2.2.3 Measurement of flow rate and calculation of permeability

The flow rate of each NTD was measured by connecting the back of the NTD to a nitrogen gas line with a pressure 15 psi above atmosphere, and then measuring the flow rate coming out from the front tip of the needle with a flow meter. The pressure of the needle inlet was assumed to be 15 psi above atmosphere while the needle outlet pressure

was assumed to be atmospheric pressure. Thus, the pressure difference between the two ends of the sorbent bed ($\Delta p$) was assumed to be 15 psi. Additionally, the viscosity of nitrogen gas ($\mu$) is $1.657\times10^{-5}$ kg/m·s, the length of sorbent bed was 1, 2, and 3 cm in accordance with the different NTDs, and the cross-sectional area of the needle ($A$) was $1.32\times10^{-7}$ $m^2$, therefore, the permeability of each needle can be calculated by substituting the value of each specific parameter into Equation (16).

## 2.3 Results and discussion

### 2.3.1 Influence of sorbent type and sorbent particle size

To compare the permeability of the NTDs packed with different materials, the flow rates of 6 types of NTDs (in triplicate) packed with CAR or DVB particles of 60/80 mesh, 80/100 mesh, and 100/120 mesh were tested and the permeabilities were calculated and compared in Table 2-1.

**Table 2-1 Permeabilities of NTDs packed with different adsorbents (n=3)**

| **Sorbent type** | **DVB** | | | **CAR** | | |
|---|---|---|---|---|---|---|
| **Mesh size** | 60/80 | 80/100 | 100/120 | 60/80 | 80/100 | 100/120 |
| **Packed mass amount (mg) (RSD (%))** | 0.413 (3.7) | 0.472 (3.0) | 0.516 (5.1) | 0.493 (4.5) | 0.565 (1.1) | 0.632 (1.2) |
| **Porosity** | 0.678 | 0.632 | 0.605 | 0.804 | 0.775 | 0.749 |
| **Flow rate (mL/min) (RSD (%))** | 88.3 (3.9) | 64.5 (3.5) | 54.6 (4.8) | 126 (2.2) | 83.4 (0.3) | 56.6 (1.5) |
| **Permeability ($10^{-5}$ $cm^2$)** | 2.32 | 1.70 | 1.44 | 3.31 | 2.19 | 1.49 |
| **Relative resistance ($1/k_p$)** | 1.00 | 1.36 | 1.61 | 1.00 | 1.51 | 2.22 |

The results shown in Table 2-1 indicate that the permeabilities of the NTDs packed with smaller particles are much smaller than for those with larger particles, due to a smaller porosity of the sorbent bed, as smaller particles can be more efficiently packed

inside a needle. Moreover, it is noted that for the same particle size and packing length, permeabilities were different for various adsorbents due to different porosities of sorbent beds caused by different pore structures and particle geometries. Thus, the permeability of the NTD could be adjusted by using appropriate sorbent particles of different sizes to get sorbent beds of various porosities.

### 2.3.2 Influence of packing length

The flow rates of the NTDs (in triplicate) packed with the same adsorbent (60/80 mesh DVB or 60/80 mesh CAR) but with different packing lengths were also tested and the permeabilities were determined, as shown in Table 2-2. A schematic illustration of the relative resistance with the increase of packing length is plotted in Figure 2-2 (next page).

**Table 2-2 Permeabilities of NTDs with different lengths of sorbent beds (n=3)**

| **Adsorbent** | **DVB** | | | **CAR** | | |
|---|---|---|---|---|---|---|
| **Packing length (cm)** | 1 | 2 | 3 | 1 | 2 | 3 |
| **Mass packed (mg)** | 0.413 | 0.729 | 1.11 | 0.493 | 0.881 | 1.27 |
| **(RSD (%))** | (3.7) | (3.5) | (5.2) | (4.5) | (5.2) | (1.2) |
| **Porosity** | 0.678 | 0.716 | 0.711 | 0.804 | 0.825 | 0.832 |
| **Flow rate (mL/min)** | 88.3 | 49.6 | 31.5 | 126 | 78.6 | 62.0 |
| **(RSD (%))** | (3.9) | (8.5) | (39.3) | (2.2) | (2.3) | (2.7) |
| **Permeability ($10^{-5}$ $cm^2$)** | 2.32 | 1.30 | 0.83 | 3.31 | 2.07 | 1.63 |
| **Relative resistance ($1/k_p$)** | 1.00 | 1.78 | 2.80 | 1.00 | 1.60 | 2.03 |

As shown in Figure 2-2, the resistance increased linearly for both DVB and CAR needles with the increase in the packing length. The intercepts represent the resistance caused by the immobilizing materials on the two sorbent ends. A comparison between the two intercepts indicates that the resistance caused by the immobilizing material was

negligible for DVB needles, but comparable to the resistance caused by 1 cm 60/80 mesh CAR sorbent bed for CAR needles, which is due to the fact that the resistance of the DVB sorbent is much larger than that of the CAR sorbent. Moreover, comparing Table 2-1 with Table 2-2, the permeability of the NTDs packed with 2 cm 60/80 mesh DVB was comparable to that of the NTDs packed with 1 cm 100/120 mesh DVB, while the permeability of the NTDs packed with 3 cm 60/80 mesh CAR was comparable to that of the NTDs packed with 1 cm 100/120 mesh CAR. From this perspective, the particle size has a more significant effect than the packing length on the permeability. However, whether it is good to pack shorter sorbent bed with smaller particles or longer sorbent bed with larger particles depends on the relative capacities and desorption efficiencies of the NTDs packed with those sorbents, which will be determined later.

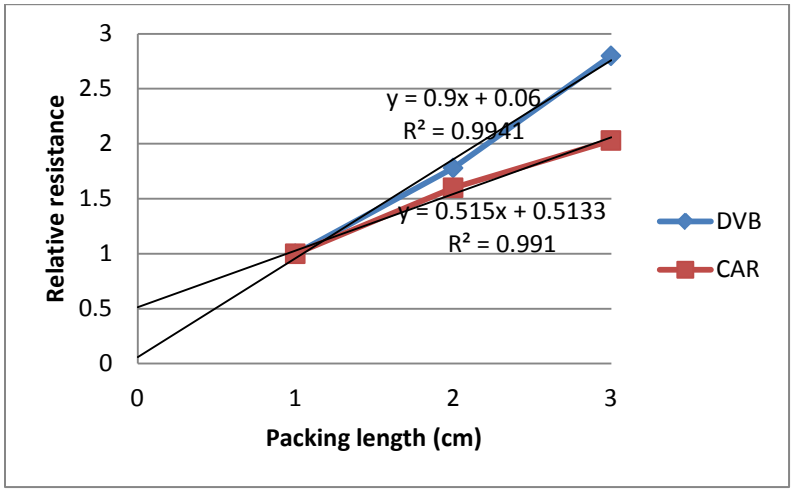


**Figure 2-2 Schematic illustration of the relative resistance with the increase of packing length for DVB and CAR needles**

### 2.3.3 Influence of immobilizing material

Glue, stainless spring wire, and glass wool are three materials commonly used in the literature to date to immobilize the sorbent bed. The holding material also has a significant effect on the permeability of an NTD. To investigate the extent of the holding material affecting the permeability, NTDs (in triplicate) packed with 60/80 mesh CAR were immobilized with glue, spring wire, glass wool, and silanized glass wool paper at the opening end. Then the flow rate of each NTD was determined experimentally under the same conditions, and the permeability was calculated and compared in Table 2-3.

**Table 2-3 Permeabilities of the NTDs held with different materials (n=3)**

| Holding material | Glue | Spring wire | Glass wool | Silanized glass wool paper |
|---|---|---|---|---|
| **Flow rate (mL/min) (RSD (%))** | 126 (2.2) | 105 (9.1) | 82.0 (30) | 9.67 (2.9) |
| **Permeability ($10^{-5}$ $cm^2$)** | 3.31 | 2.76 | 2.16 | 0.25 |

As shown in Table 2-3, the NTDs immobilized with glue still presented a great advantage over the NTDs packed with other materials for the much larger permeability. It is reasonable that the use of glue binds the particles at the top layer together and also strongly binds the top layer particles to the surface of the needle without significantly blocking the pores. It should be noted that the amount of glue applied to the sorbent bed should be extremely small in order to avoid a significant reduction of the permeability, or even the blockage of the needle. It should also be noted that the excess use of glue might increase the amount of potential thermal decomposition product and contaminants from glue during desorption, which cannot be avoided but can be minimized after long time conditioning.

## 2.4 Conclusion

The permeabilities of NTDs packed with different adsorbents of different sizes were determined experimentally, and the influence of immobilizing material was also investigated. As seen in the results, the permeability of the needle increased with the increase in particle size, and proportionally decreased with the increase in packing length. To obtain a higher permeability, larger particles should be used, but larger particles are, in most cases, less efficiently packed inside the sorbent bed, resulting in lower extraction capacity and efficiency. Thus, the selection of particle size will be a compromise between capacity and flow rate, which will be determined in subsequent work. It is also noted that the permeability was affected by the immobilizing material at the two sorbent ends and that glue still showed the smallest resistance over other immobilizing materials.

# Chapter 3 Evaluation and optimization of needle capacity relative to particle size

## 3.1 Introduction

Theoretically, the capacity of the NTD is closely related to the kinetics of the sampling process, which could be described by Equation (6) (Page 19). Under the same linear flow rate, a longer period of time to reach breakthrough reveals the NTD has a larger capacity. A detailed explanation of Equation (6) with different *n*, *k*, *u* is illustrated in Figures 3-1 to 3-3, from which we can see that breakthrough is strongly related to *n*, *k*, and *u*. However, as shown in Figures 3-1 and 3-2, with a two orders of magnitude increase of *n*, the time required for breakthrough is increased by only 50%, while the breakthrough exhibits the same order of increase with the same increase of *k*. This is reasonable since the retention factor (reflected by *k*) determines the capacity (reflected by the breakthrough time under a specific flow rate) of the adsorbent to retain the analytes, while *n* only affects the concentration distribution of the front. As can be observed in Figure 3-3, the distribution of the frontal concentration is independent of *u*, and the decrease of *u* results in an increase of the breakthrough time *t*. However, the product of *u* and *t* at breakthrough, which corresponds to the breakthrough volume, is the same for different *u*, indicating the capacity of the adsorbent is independent of the sampling rate. Nevertheless, according to Equations (1) and (2), *u* will affect *n* and consequently affect the concentration distribution of the front, resulting in a different capacity of the NTD. Thus, there is an optimal *u* for the sampling process.

The objective of this work is to validate the proposed theory and optimize the needle capacity with respect to sorbent particle size.

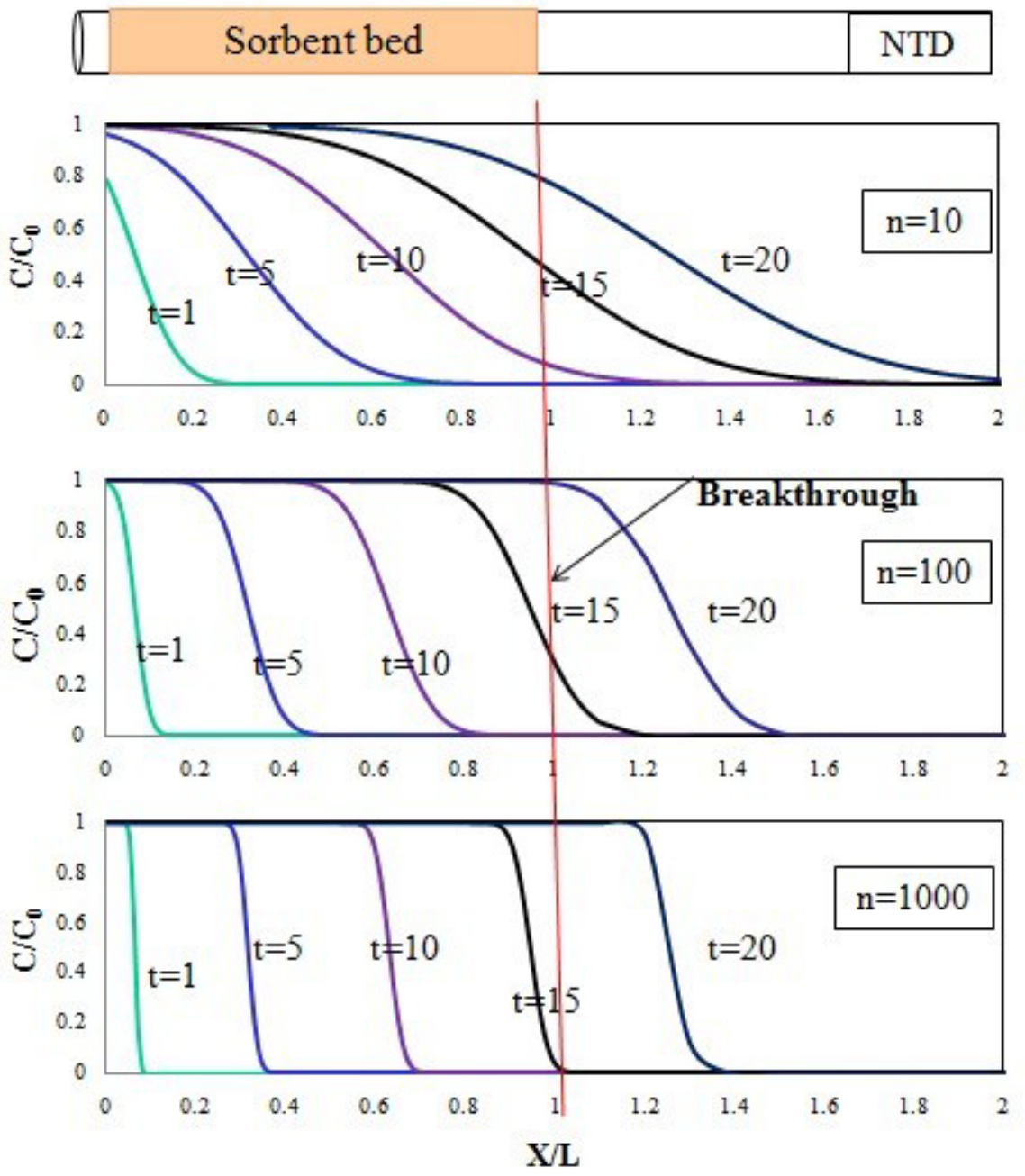


**Figure 3-1 The concentration profile of the elution front along the *x*-axis at different time t (seconds) with different *n* (*u*=63 cm/s, *k*=1000)**

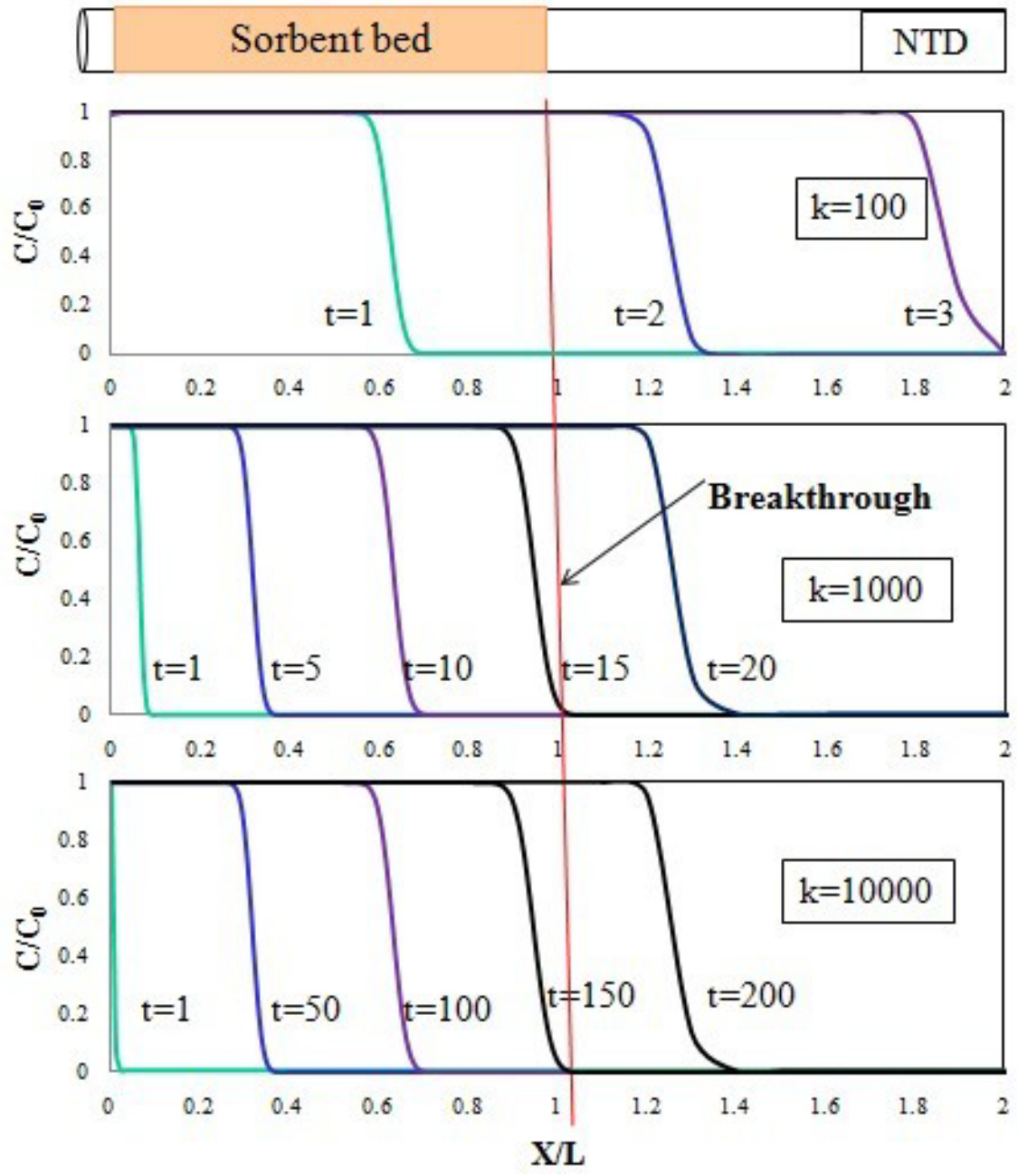


**Figure 3-2 The concentration profile of the elution front along the *x*-axis at different time *t* (seconds) with different *k* (*u*=63 cm/s, *n*=1000)**

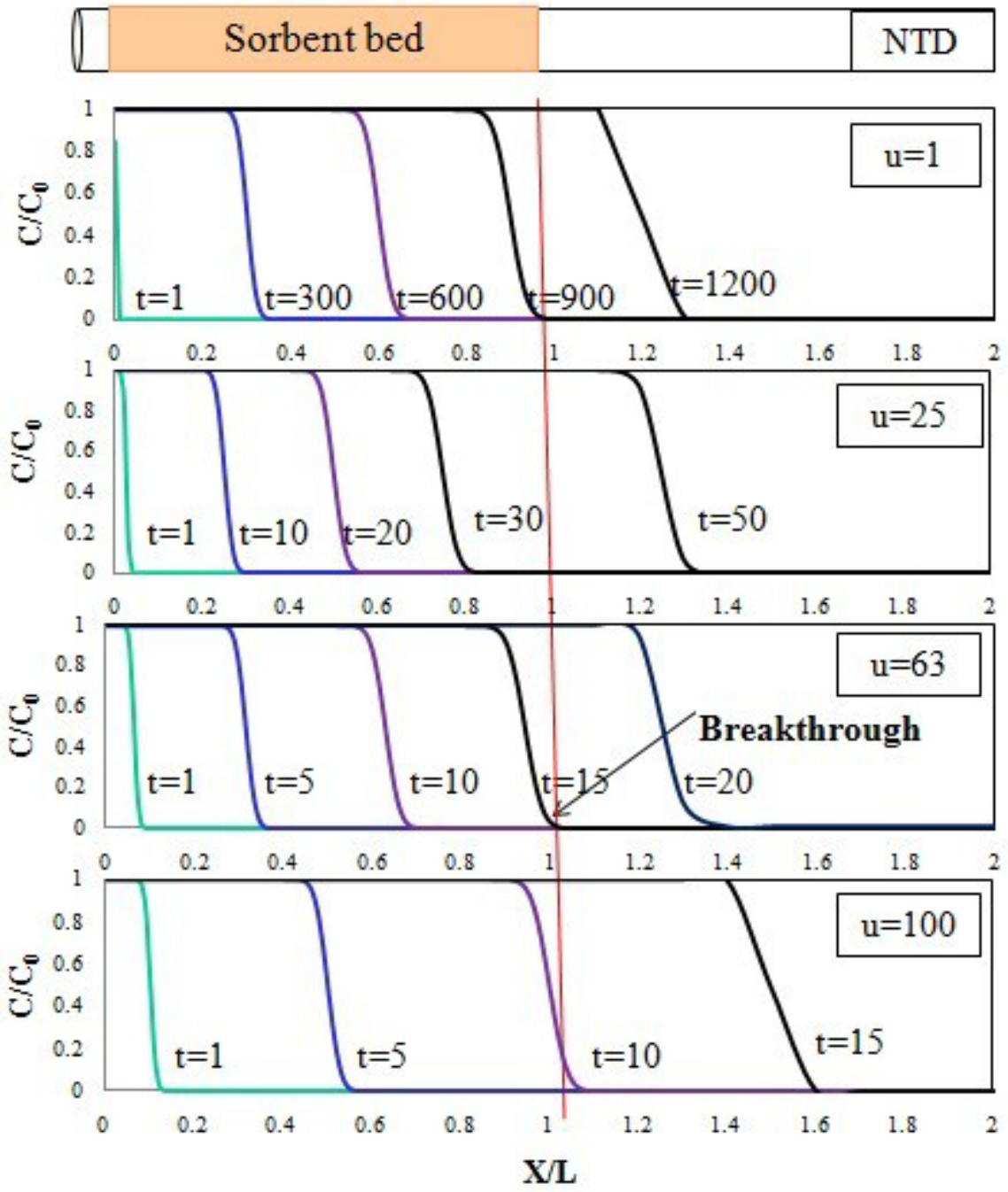


**Figure 3-3 The concentration profile of the elution front along the *x*-axis at different time *t* (seconds) with different *u* (cm/s) (*n*=1000, *k*=1000)**

## 3.2 Experimental section

### 3.2.1 Chemicals and materials

Toluene, ethylbenzene, and *o*-xylene (TEX compounds) were purchased from Sigma-Aldrich (Bellefonte, PA, USA). The bi-directional syringe pump was purchased from Kloehn (Las Vegas, NV, USA). The 1 mL gas-tight syringe was purchased from Hamilton (Reno, NV, USA). Other chemicals and materials used were the same as Section 2.2.1.

### 3.2.2 Gas standard generator

A standard gas generator (model 491 M-B, Kin-Tech Laboratories, LaMarque, TX, USA) was used to generate the TEX standard gases with desired concentrations. The self-made permeation tubes were placed inside a glass chamber held in a temperature-controlled oven and swept with a controllable constant flow of compressed air. Different concentrations of TEX compounds were obtained by adjusting both the permeation chamber temperature and the air flow rate.

### 3.2.3 Preparation of NTDs

The NTDs were prepared using a procedure that has already been described in Section 2.2.2. The sorbent beds packed inside the needles for this work were 1 cm 60/80 mesh Tenax, 1 cm 60/80 mesh DVB, 1 cm 80/100 mesh DVB, 1 cm 100/120 mesh DVB, 1 cm 60/80 mesh CAR, 1 cm 80/100 mesh CAR, and 1 cm 100/120 mesh CAR, respectively. All the sorbent beds in the NTDs were immobilized with glue at the opening ends. After packing, the NTDs were conditioned in a GC injector for 2 hours with helium

gas continuously flowing through the needle. The conditioning temperature was 250 °C for the DVB needles, and 300 °C for both the Tenax needles and the CAR needles.

### 3.2.4 Sampling and desorption

For TEX sampling, the NTD was connected to the sampling pump and a specific volume of the gaseous sample was pumped through the needle from the gas standard generator at a flow rate of 5 mL/min. After sampling, the NTD was connected to a 1 mL gas-tight syringe filled with a certain volume of helium, and then introduced into a GC injector for desorption. The helium was consistently pushed out to assist the desorption during the whole desorption period. For NTDs packed with DVB, the needle was injected into the hot GC injector at 250 °C for 1 min with the assistance of 0.3 mL helium; For CAR NTDs, the needle was injected into the GC injector at 300 °C for 2 min with the assistance of 0.5 mL helium; For Tenax NTDs, the needle was injected into the GC injector at 300 °C for 1 min with the assistance of 0.3 mL helium.

### 3.2.5 Instrumentation

A Varian CP-3800 gas chromatograph with a flame ionization detector (GC/FID) and a DB-5HS column (30 m × 0.25 mm × 0.25 μm) (J&W Scientific, Mississauga, ON, Canada) was used to separate and analyze the target compounds. The injector temperature was 250 °C for DVB needles, and 300 °C for CAR and Tenax needles. The injection was made in splitless mode with an SPME liner. The initial oven temperature was set at 30 °C and held for 1 min, then ramped up to 140 °C at a rate of 25 °C/min, and held at 140 °C for 0.5 min.

## 3.3 Results and discussions

### 3.3.1 Theory validation

To validate the theory, two types of NTDs packed with 1 cm 60/80 mesh Tenax GC and 1 cm 60/80 mesh DVB in duplicate were used to sample TEX compounds at concentrations of 1.22 ppb, 1.67 ppb and 0.167 ppb, from the gas standard generator, and the experimental results are shown in Figures 3-4 and 3-5.

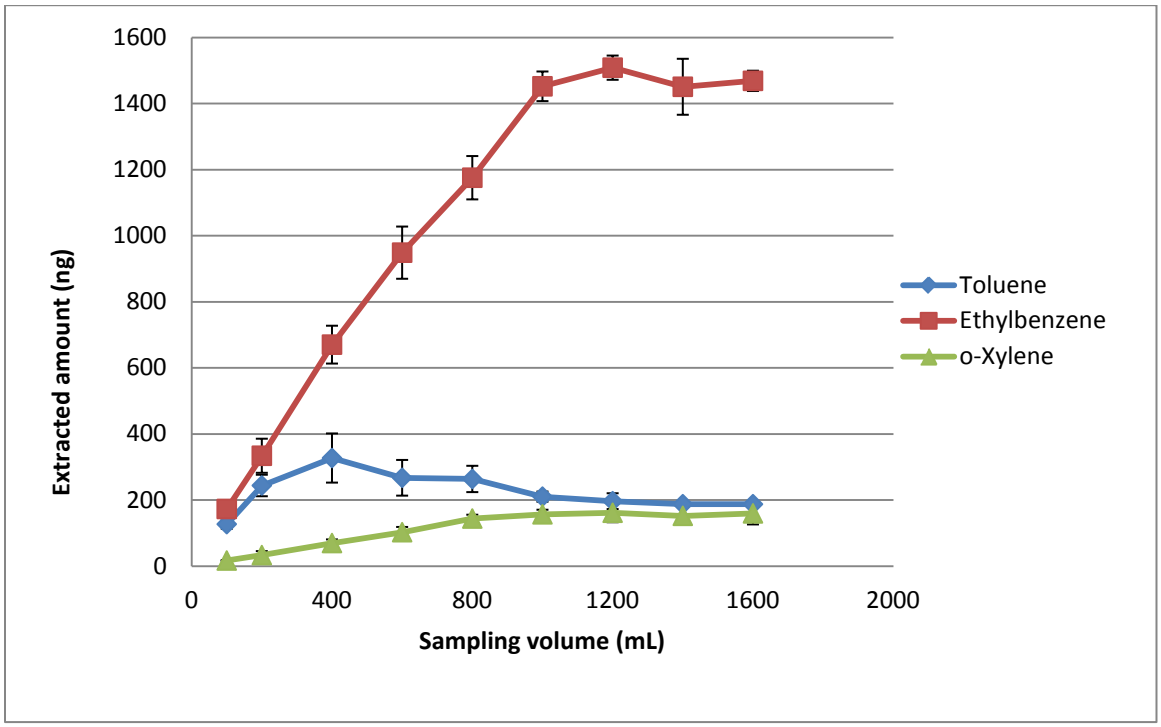


**Figure 3-4 The breakthrough volumes of TEX compounds using NTDs packed with 60/80 mesh DVB (n=4: two needles, duplicate for each needle)**

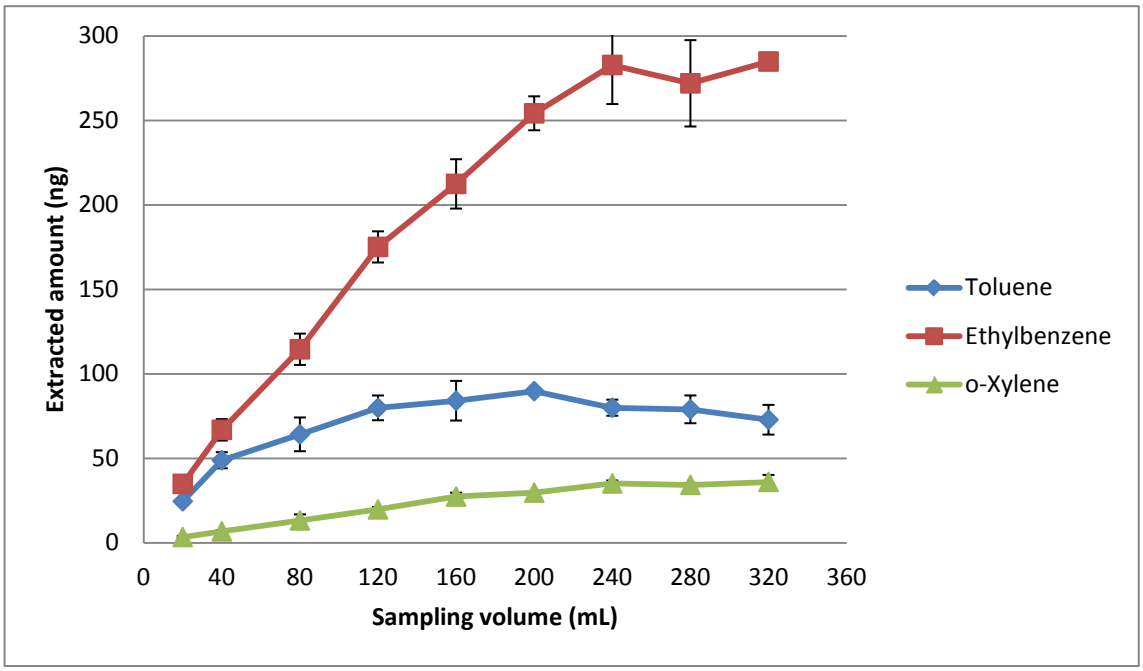


**Figure 3-5 Breakthrough volumes of TEX compounds using NTDs packed with 60/80 mesh Tenax GC (n=4, two needles, duplicate for each needle)**

Assuming that the breakthrough volume has been reached when the extracted amount of a compound is 5% less than the expected amount, the experimental breakthrough volume was determined as follows. First, for each compound, using the extraction amount profile (Figures 3-4 and 3-5), a line was plotted as the expected extraction line without breakthrough using the first few experimental data points and the expected extraction amount at each data point was calculated. Second, the experimental extraction amount was compared with the expected amount. If at one point, the experimental amount was less than 95% of the expected extraction amount, then the experimental amount was substituted into the linear equation of the plotted line to get the breakthrough volume. The breakthrough volumes are presented in Table 3-1.

**Table 3-1 Experimental breakthrough volumes of each compound for two types of needles**

| Sorbent | | DVB | Tenax GC |
|---|---|---|---|
| **Breakthrough volumes (mL)** | Toluene | 286 | 55 |
| | Ethylbenzene | 742 | 156 |
| | *o*-Xylene | 958 | 191 |

The theoretical breakthrough volume of each compound for each type of NTDs could be determined by the procedure below.

For the NTDs packed with a certain type of material, the retention factor *k* may be calculated as follows:

$$k = K_{es}\frac{s_e}{V_v} = \frac{C_s}{C_0}\frac{S_e}{V_v} \qquad (17)$$

Where $C_sS_e$ is equal to the extracted amount on the sorbent at equilibrium, which can be determined experimentally. As previously mentioned, $C_0$ is the initial concentration of the analyte in the sample, $V_v$ is the void volume of the sorbent bed.

For Equation (2), T has the following relationship with porosity ∅ [47],

$$T = 1 - 1/2ln\emptyset \qquad (18)$$

Thus, we obtain

$$D = \frac{1}{(1-\frac{1}{2}ln\emptyset)^2}D_M + (1-\frac{1}{2}ln\emptyset)d_p u \qquad (19)$$

When Equation (18) is substituted into Equation (1), we obtain

$$n = \frac{1}{2}\frac{uL}{\frac{1}{(1-\frac{1}{2}ln\emptyset)^2}D_0 + (1-\frac{1}{2}ln\emptyset)d_p u} \qquad (20)$$

By substituting the gas diffusion constants of toluene, ethylbenzene, and *o*-xylene ($D_{\text{toluene}}$=0.085 cm$^2$/sec, $D_{\text{ethylbenzene}}$=0.076 cm$^2$/sec, and $D_{o\text{-xylene}}$=0.073 cm$^2$/sec) and the

corresponding $u$, $L$, $d_p$ into Equation (20), the theoretical plate number is obtained. Then the breakthrough volume can be determined by Equation (14). Table 3-2 presents the theoretical predicted results.

**Table 3-2 Theoretical calculated results for breakthrough volumes**

| **Adsorbent** | | **DVB** | **Tenax GC** |
|---|---|---|---|
| **Mesh size** | | 60/80 | |
| $D_p$ **(μm)** | | 215 | 215 |
| Ø | | 0.662 | 0.739 |
| $L$ **(cm)** | | 1 | 1 |
| $u$ **(cm/sec)** | | 95.3 | 85.4 |
| $n$ | **Toluene** | 18.8 | 19.6 |
| | **Ethylbenzene** | 18.9 | 19.7 |
| | ***o*-Xylene** | 18.9 | 19.7 |
| $k$ | **Toluene** | 1.79E+05 | 6.49E+04 |
| | **Ethylbenzene** | 1.01E+06 | 1.72E+05 |
| | ***o*-Xylene** | 1.08E+06 | 2.15E+05 |
| **BTV (mL)** | **Toluene** | 143 | 58 |
| | **Ethylbenzene** | 807 | 154 |
| | ***o*-Xylene** | 863 | 193 |

A comparison between the theoretical predicted results and the experimental values is shown in Table 3-3.

**Table 3-3 Comparison between the experimental BTV values and the theoretical predictions**

| **Sorbent** | **DVB** | | | **Tenax GC** | | |
|---|---|---|---|---|---|---|
| **Compounds** | Toluene | Ethylbenzene | *o*-Xylene | Toluene | Ethylbenzene | *o*-Xylene |
| **Experimental BTV (mL)** | 286 | 742 | 958 | 55 | 156 | 191 |
| **Theoretical BTV (mL)** | 143 | 807 | 863 | 58 | 154 | 193 |
| **Relative error (%)** | -50.0 | 8.8 | -9.9 | 5.5 | -1.3 | 1.0 |

As is seen in Table 3-3, the theoretical predictions show good agreement with the experimental results, except for toluene using DVB-NTDs. This is due to the competitive adsorption of the TEX compounds on the DVB sorbent bed. With an increase of the

sampling volume, the extracted amount of toluene initially increased, and decreased after reaching the maximum sampling volume, which is also shown in Figure 3-5. It should be noted that the competitive adsorption would induce an underestimation of the BTV for the compounds with lower affinity towards a certain sorbent, but in practice, the maximum sampling volume is determined by the compound with the smallest BTV. Thus, it is still practical to use the theoretical model to predict the maximum sampling volume of an NTD. It should also be noted that the theory is based on an equilibrium assumption: there should be no saturation of the adsorbent when breakthrough occurs. To verify that the condition of no saturation of the adsorbent has been met in the experiment above, the same types of NTDs were used to extract TEX samples with concentrations of 0.61 ppb, 0.84 ppb, and 0.08 ppb. The observed breakthrough volumes were almost the same as for the above experiment indicating the equilibrium conditions were met in both cases.

A low analyte concentration is the prerequisite for equilibrium extraction. When NTDs are used to sample target analytes at high concentrations, saturation of the sorbent before equilibrium might happen, which would induce early breakthrough, as illustrated in Figures 3-6 and 3-7. However, the pre-saturation conditions can be treated as an alternative type of “equilibrium condition”, which in some cases can be used to evaluate and optimize the NTD, such as the investigation of the capacities of different needle types.

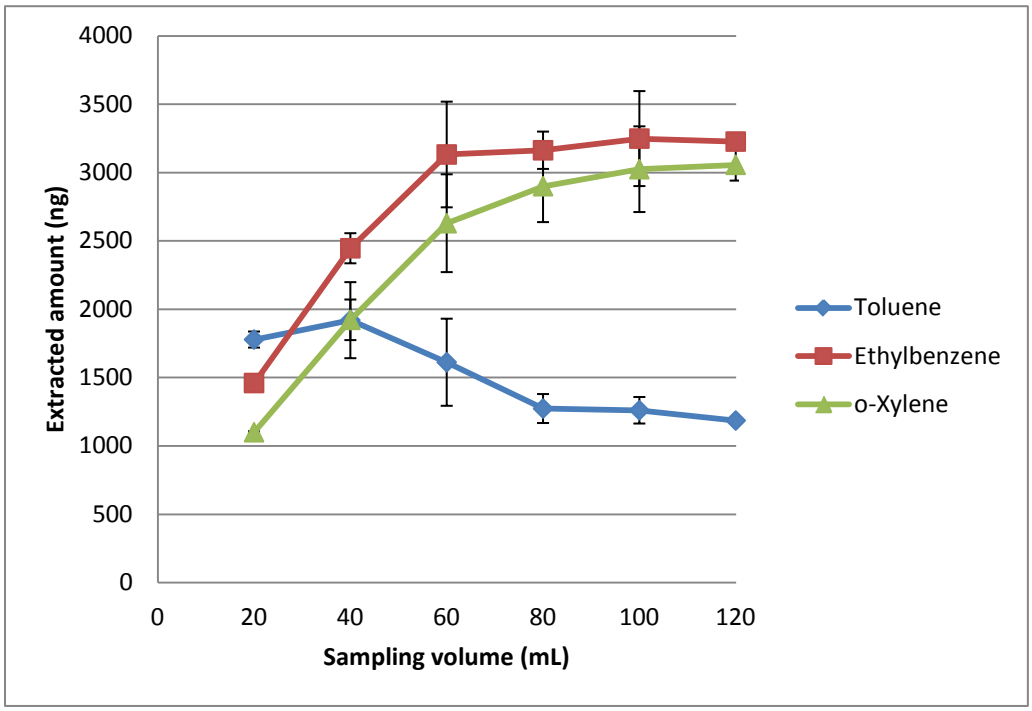


**Figure 3-6 Breakthrough volumes of TEX compounds at high concentrations using NTDs packed with 60/80 mesh DVB (n=4, two needles, duplicate for each needle)**

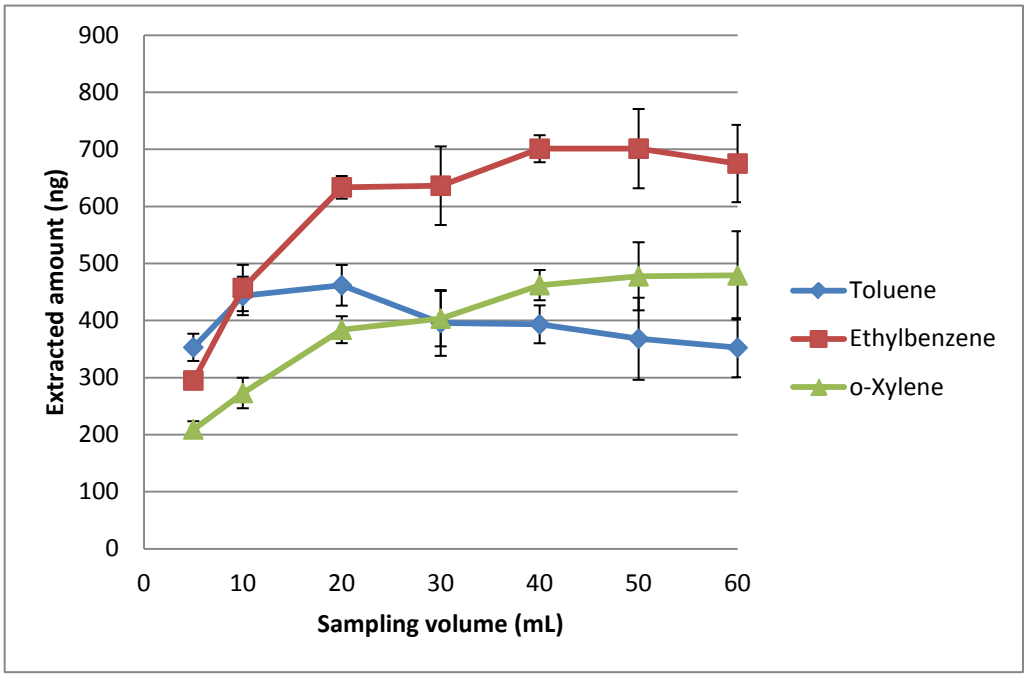


**Figure 3-7 Breakthrough volumes of TEX compounds at high concentrations using NTDs packed with 60/80 mesh Tenax GC (n=4, two needles, duplicate for each needle)**

### 3.3.2 Comparison of the capacities of NTDs packed with particles of different sizes

For particles with a smaller size, the particles may be more efficiently packed with lower inter-particle porosity. Thus, in principle, an NTD packed with smaller particles should have a larger capacity due to a larger amount of the adsorbent packed, and a higher theoretical plate height. To investigate the influence of particle dimensions on the capacity of a NTD, six types of NTDs (in duplicate) packed with 1 cm CAR or DVB of 60/80 mesh, 80/100 mesh and 100/120 mesh were used to sample TEX from the gas standard generator and the breakthrough volumes were determined. A detailed comparison of the breakthrough volumes for NTDs packed with the same adsorbent but with different sizes is shown in Table 3-4.

**Table 3-4 Breakthrough volume and the absolute extracted amount for each type of NTD (n=4: two needles, duplicate for each needle)**

| **Adsorbent** | | **DVB** | | | **CAR** | | |
|---|---|---|---|---|---|---|---|
| **Mesh size** | | 60/80 | 80/100 | 100/120 | 60/80 | 80/100 | 100/120 |
| **Mass packed (mg)** | | 0.413 | 0.457 | 0.516 | 0.493 | 0.565 | 0.632 |
| **Extraction phase volume ($mm^3$)** | | 0.409 | 0.452 | 0.511 | 0.247 | 0.283 | 0.316 |
| **BTV (mL)** | Toluene | 53 | 69 | 77 | 280 | 320 | 320 |
| | Ethylbenzene | 133 | 164 | 166 | 290 | 350 | 400 |
| | *o*-Xylene | 149 | 177 | 187 | 290 | 370 | 400 |
| **Extracted amount before breakthrough (ng)** | Toluene | 2141 | 2788 | 3111 | 23576 | 26944 | 26944 |
| | Ethylbenzene | 4642 | 5724 | 5793 | 18792 | 22680 | 25920 |
| | *o*-Xylene | 2995 | 3558 | 3759 | 13978 | 17834 | 19280 |
| **Relative ratio of BTVs** | Toluene | 1 | 1.30 | 1.45 | 1 | 1.14 | 1.14 |
| | Ethylbenzene | 1 | 1.23 | 1.25 | 1 | 1.21 | 1.38 |
| | *o*-Xylene | 1 | 1.19 | 1.26 | 1 | 1.28 | 1.38 |

As shown in Table 3-4, the capacity of the NTDs for TEX compounds exhibited 20% to 40% increases with the decrease of particle size. The breakthrough volume ratio

of each type of NTD packed with the same adsorbent but different mesh size may be estimated by Equation (14) as well. For the NTDs packed with the same material, the distribution constant $K_{es}$ should be the same under the same experimental conditions. Then the retention factor $k$ is proportional to $\frac{V_e}{V_v}$. For the adsorbent used, $k$ is usually very large under experimental temperature (room temperature), thus, $1 + k \approx k \propto \frac{V_e}{V_v}$.

By substituting the diffusion constants of each compound and the corresponding $u$, $L$, and $d_p$ into Equation (20), the table below is obtained.

**Table 3-5 Different *n* values with respect to NTDs packed with different adsorbent**

| **Adsorbent** | | **DVB** | | | **CAR** | | |
|---|---|---|---|---|---|---|---|
| **Mesh size** | | 60/80 | 80/100 | 100/120 | 60/80 | 80/100 | 100/120 |
| $D_p$ **(μm)** | | 210 | 163 | 137 | 210 | 163 | 137 |
| Ø | | 0.678 | 0.632 | 0.605 | 0.804 | 0.775 | 0.749 |
| $L$ **(cm)** | | | 1 | | | 1 | |
| $u$ **(cm/sec)** | | 93.1 | 99.9 | 104.3 | 78.5 | 81.4 | 84.3 |
| $n$ | Toluene | 19.4 | 24.3 | 28.3 | 20.7 | 26.0 | 30.4 |
| | Ethylbenzene | 19.5 | 24.3 | 28.4 | 20.8 | 26.2 | 30.5 |
| | *o*-Xylene | 19.5 | 24.4 | 28.4 | 20.8 | 26.2 | 30.6 |

Substituting $n$, Ø, and $u$ into Equation (14), we obtained the ratios of the breakthrough volumes for TEX with different NTDs as are shown in Table 3-6.

**Table 3-6 Theoretical ratio of breakthrough volumes (BTVs) for TEX**

| **Adsorbent** | | **DVB** | | | **CAR** | | |
|---|---|---|---|---|---|---|---|
| **Mesh size** | | 60/80 | 80/100 | 100/120 | 60/80 | 80/100 | 100/120 |
| **Theoretical Ratio of BTVs** | Toluene | 1.00 | 1.17 | 1.28 | 1.00 | 1.18 | 1.33 |
| | Ethylbenzene | 1.00 | 1.17 | 1.28 | 1.00 | 1.18 | 1.33 |
| | *o*-Xylene | 1.00 | 1.17 | 1.28 | 1.00 | 1.18 | 1.33 |

Comparing the data presented in Table 3-6 with the ratios from Table 3-4, the theoretical predictions are in good agreement with the experimental ratios with less than 5% deviation for most predictions. The major deviation comes from the simplification for the calculation of apparent diffusion constant in Equation (2). The diffusion caused by the mass transfer through the extraction phase was neglected in Equation (2), which induced an underestimated apparent diffusion constant *D* and consequently led to an overestimated theoretical plate number *n* and subsequently an underestimated ratio. Moreover, as shown in Table 3-6, the theoretical ratio is independent of the adsorbent used, which is also due to the disregard for mass transfer through the extraction phase. In addition, since the sampling is always conducted at a high flow rate in real applications for NTD, multipath diffusion ($Td_pu$) dominates the diffusion process. Thus, it is reasonable that the theoretical ratios of BTVs for the TEX compounds are almost identical as seen in Table 3-6.

Equation (14) is very useful when predicting the relative BTVs with respect to different adsorbents with different sizes and packing densities. It is also shown in Equation (14) and Figures 3-1 to 3-3, that choosing a proper adsorbent with a relatively high *K* value so as to get a high *k* value is more important than optimizing the particle size and packing density.

To confirm that the relative capacities of the NTDs packed with different adsorbents under different concentrations are similar, the breakthrough volumes of NTDs packed with DVB of different sizes were tested under different concentrations. The results are shown in Table 3-7. The experimental ratios are in good agreement with the theoretical predictions. As shown in the results, the breakthrough volumes decreased with

the increase of the analyte concentrations at pre-equilibrium saturation condition. At low concentration, the breakthrough volume could go up to 1000 mL, which is extremely important for NTD as an exhaustive sampler. In environmental trace analysis, the concentrations of the analytes may be much lower than 1 ppb; the large capacity of the NTDs allows collection of several hundred millilitres of the sample without breakthrough. With the use of segmented adsorbents inside the needle, NTD is able to extract a much wider range of compounds, as demonstrated previously [31,48].

**Table 3-7 Relative ratio of the capacities of NTDs packed with DVB of different sizes under different concentrations (n=4: two needles, duplicate for each needle)**

| **Particle size (mesh)** | | | | **60/80** | **80/100** | **100/120** |
|---|---|---|---|---|---|---|
| **Ratios of BTVs** | **Toluene** | Low (0.58 ppb) | BTV (mL) (Relative ratio) | 278 (1.00) | 356 (1.28) | 365 (1.31) |
| | | Medium (9.60 ppb) | BTV (mL) (Relative ratio) | 134 (1.00) | 183 (1.37) | 200 (1.49) |
| | | High (40.4ppb) | BTV (mL) (Relative ratio) | 53 (1.00) | 69 (1.30) | 77 (1.45) |
| | **Ethylbenzene** | Low (2.26 ppb) | BTV (mL) (Relative ratio) | 588 (1.00) | 737 (1.25) | 782 (1.33) |
| | | Medium (7.27 ppb) | BTV (mL) (Relative ratio) | 295 (1.00) | 355 (1.20) | 398 (1.35) |
| | | High (34.9 ppb) | BTV (mL) (Relative ratio) | 133 (1.00) | 177 (1.23) | 187 (1.25) |
| | ***o*-Xylene** | Low (0.23 ppb) | BTV (mL) (Relative ratio) | 974 | Up to 1000 mL without breakthrough | |
| | | Medium (5.69 ppb) | BTV (mL) (Relative ratio) | 306 (1.00) | 366 (1.19) | 406 (1.33) |
| | | High (20.1 ppb) | BTV (mL) (Relative ratio) | 149 (1.00) | 177 (1.19) | 187 (1.26) |

## 3.4 Conclusion

The fundamental parameters of NTDs with respect to different packing materials and particle dimensions were investigated and the proposed theory was validated. It was found that experimental results were in good agreement with the theoretical predictions. Smaller particles could be more efficiently packed inside the needle, resulting in a higher packing density and consequently a higher extraction capacity of the NTD. Comparing the trend of capacity and resistance with the decrease of sorbent particles size, it is noted that resistance increases much faster than capacity. Thus, it would be preferable to pack NTDs with longer sorbent beds using larger particles (i.e. 2 cm 60/80 mesh DVB) rather than pack the NTDs with shorter sorbent beds using smaller particles (i.e. 1 cm 100/120 mesh DVB), especially for active sampling. Future work will focus on investigating the influence of particle size on the desorption efficiency of the needle. By comparing the permeability, the capacity and the desorption efficiency, the NTD with the appropriate packing will be optimized.

# Chapter 4 Desorption efficiency investigation

## 4.1 Introduction

Desorption efficiency is strongly related to the affinity of the adsorbent, the permeability, the porous structure of the sorbent bed, and the desorption method used. In this work, the desorption efficiencies of NTDs packed with different adsorbents, and the same adsorbents of different particle sizes, were investigated and compared. The desorption efficiencies of different desorption methods were compared as well.

## 4.2 Experimental section

### 4.2.1 Chemicals and materials

*n*-hexane and *n*-decane were purchased from Sigma-Aldrich (Bellefonte, PA, USA). Other chemicals and materials used were the same as Section 3.2.1.

### 4.2.2 Gas standard generator

The same gas standard generator (as described in Section 3.2.2) was used to generate *n*-hexane, toluene, ethylbenzene, *o*-xylene, and *n*-decane (VOCs) standard gases with desired concentrations. The operation procedure was the same as previous described in Section 3.2.2 except that another two permeation tubes containing *n*-hexane and *n*-decane respectively were placed into the glass chamber as well to generate *n*-hexane and *n*-decane.

### 4.2.3 Preparation of NTDs

The packing process for each needle was the same as the procedure described in Section 2.2.2. The sorbent beds used were 1 cm 60/80 mesh DVB, 1 cm 80/100 mesh DVB, 1 cm 100/120 mesh DVB, 1 cm 60/80 mesh CAR, 1 cm 80/100 mesh CAR, and 1 cm 100/120 mesh CAR. All the sorbent beds in the NTDs were immobilized with glue at the opening ends. To condition, the packed needle was injected into a hot GC injector with an external helium gas flowing for 2 hours. The injector temperature was 250 °C for DVB needles and 300 °C for CAR needles.

### 4.2.4 Sampling and desorption

#### *4.2.4.1 Sampling*

For VOC sampling, the NTD was connected to the sampling pump, and 50 mL of the gaseous sample was pumped through the needle from the gas standard generator at a flow rate of 5 mL/min. The concentrations of the compounds were 18.2 ng/mL for hexane, 10.4 ng/mL for toluene, 7.6 ng/mL for ethylbenzene, 6.0 ng/mL for *o*-xylene, and 4.2 ng/mL for *n*-decane.

For PAH sampling, 10 mL of sample was pumped through the needle at a flow rate of 5 mL/min from the headspace of a 20 mL vial filled with 20 mg solid pyrene and 20 mg solid anthracene.

#### *4.2.4.2 Desorption*

##### *4.2.4.2.1 Comparing desorption efficiencies of different NTDs by thermal expansion*

To compare the desorption efficiencies of NTDs packed with DVB particles of different mesh sizes by thermal expansion desorption, each DVB-NTD was injected into the GC injection port for 0.3 min for the first desorption. Then, the NTD was connected to a gas-tight syringe filled with 0.3 mL helium and injected into the hot GC injector again for 1 min. During desorption, the 0.3 mL helium were slowly and consistently pushed out to assist the desorption. After the second desorption, no carryover was found and the carryover percentage for each type of needle, for each compound, was calculated by dividing the peak area of the second desorption by the sum of the total peak area of the first and second desorption. The desorption procedure for each CAR-NTD was similar, with slight differences in that the first desorption time was 1 min, and the second desorption was 2 min with 0.5 mL helium inside the syringe, in order to get better desorption efficiency since CAR sorbent is much stronger than DVB sorbent.

##### *4.2.4.2.2 Desorption efficiencies of different NTDs by carrier gas assisted desorption*

To compare the desorption efficiencies of different types of NTDs packed with DVB particles of different sizes by carrier gas assisted desorption, a DVB-NTD was connected to a gas-tight syringe filled with 0.3 mL helium. Then the NTD was injected into the GC injector for 1 min and 0.3 mL helium was slowly and consistently pushed out during 1 min. After the first desorption, the same procedure was repeated to determine the carryover. The desorption procedure for a CAR-NTD was the same, except that 0.5 mL helium was used inside the syringe and the desorption time was 2 min for the second desorption.

#### *4.2.4.2.3 Comparing desorption efficiencies of NTDs assisted with different external gases during desorption*

The procedures for both DVB and CAR NTDs were the same as described in Section 4.2.4.2.2, except that for the first desorption, air and nitrogen were also used as the external gas for comparing the desorption efficiency with helium-assisted desorption. For the second desorption, the procedure was the same, except that only helium was used as the assisting gas for desorption.

### 4.2.5 Instrumentation

A Varian CP-3800 gas chromatograph/flame ionization detector (GC/FID) fitted with a DB-5HS column (30 m × 0.25 mm × 0.25 μm) (J&W Scientific, Mississauga, ON, Canada) was used to separate and analyze the target compounds. The injector temperature was 250 °C for DVB needles and 300 °C for CAR needles. The injection was made in splitless mode with an SPME liner. For VOC analysis, the initial oven temperature was set at 30 °C and held for 1 min, then ramped up to 140 °C at a rate of 25 °C/min, and held at 140 °C for 0.5 min. For PAH analysis, the initial oven temperature was 40 °C and held for 1 min, then ramped up to 280 °C at 40 °C/min and held for 2 min.

## 4.3 Results and discussion

### 4.3.1 Influence of permeability on desorption efficiency

The desorption efficiency of the NTD is affected by various factors, including the permeability of the sorbent bed, the affinity of the adsorbent, the desorption method, and the needle trap design. To investigate the influence of permeability on the desorption efficiency, the carryover percentages of the NTDs packed with 60/80 mesh or 80/100

mesh DVB of the same packing density, but immobilized with different amount of glue to obtain different permeabilities, were investigated, and the results are shown in Figure 4-1. For the same type of needle with the same structure, the carryover decreased with the increase in the permeability. This could be explained by NTDs with large permeability allowing gas flow through the sorbent bed with less resistance, which consequently resulted in more efficient delivery of the desorbed analytes during desorption. In addition, as shown in Figure 4-1-A, there was no significant decrease of the carryover percentage when the permeability was high.

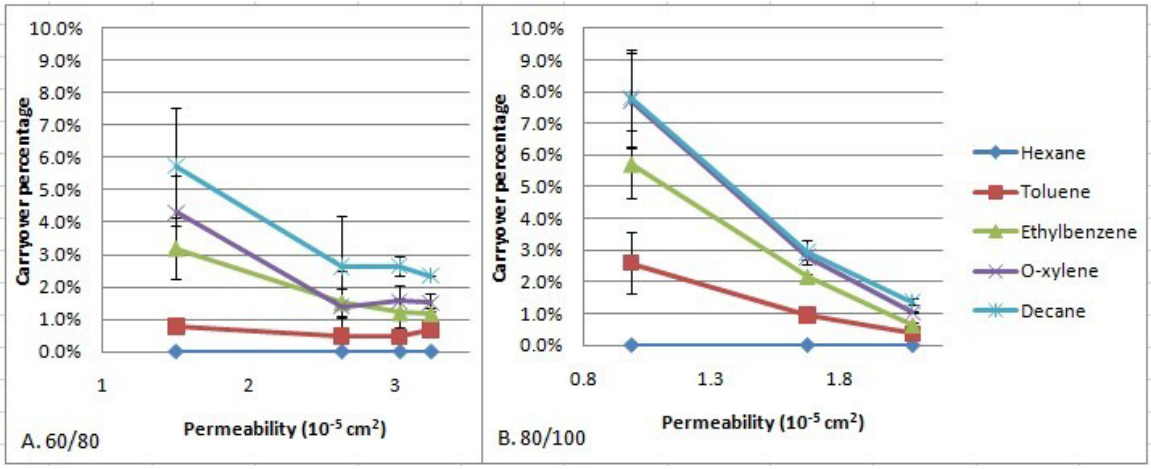


**Figure 4-1 Carryover percentages of different types of NTDs with different permeabilities**

### 4.3.2 Influence of sorbent particle size on desorption efficiency

To investigate the desorption efficiencies of the NTDs packed with adsorbents of different sizes, NTDs packed with 1 cm DVB or CAR of 60/80 mesh, 80/100 mesh, and 100/120 mesh, respectively, were tested, and the results are shown in Figures 4-2 and 4-3. To observe a higher carryover percentage, the desorption time was 0.3 min for the DVB NTDs and 2 min for the CAR NTDs.

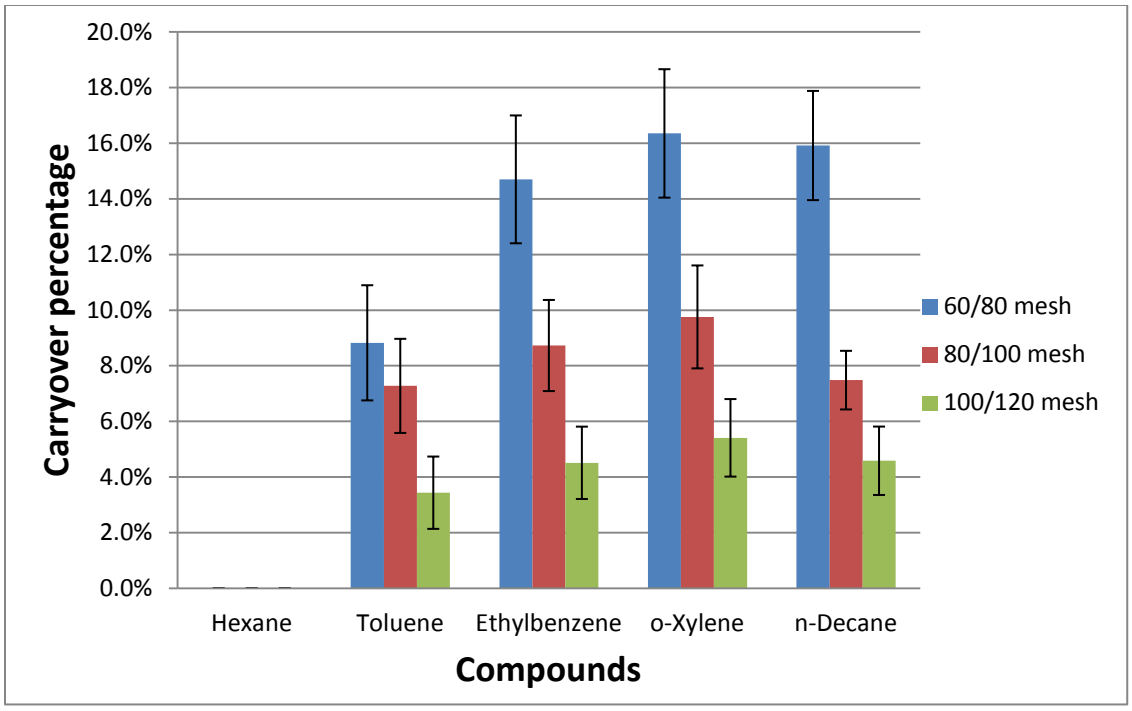


**Figure 4-2 Carryover percentages of NTDs packed with 1 cm DVB of different sizes with thermal expansion desorption (n=12: three needles, quadruplicate)**

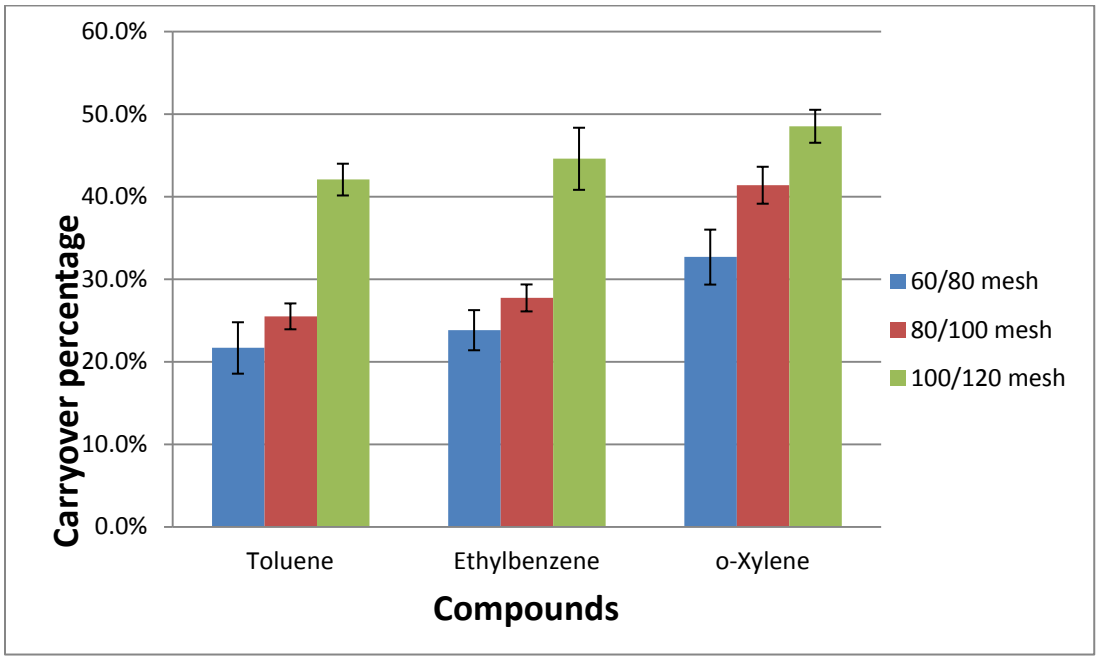


**Figure 4-3 Carryover percentages of NTDs packed with 1 cm CAR of different sizes with thermal expansion desorption (n=8: two needles, quadruplicate)**

As shown in Figures 4-3 and 4-4, the carryover of the CAR-NTDs increased with the decrease of particle size, but the DVB-NTDs packed with larger particles exhibited larger carryover percentages. To explain this phenomenon, some concepts need to be introduced first. For NTDs packed with porous particles, the pores inside the needles consisted of intra-particle pores—pores inside the particles and inter-particle pores—pores between particles. The pores of both types formed the multipath channels that allowed the gas flow to pass. The ease of the flow passing through the channels was determined by the number of these channels, which can be expressed as porosity from the macroscopic point of view. The easiness was also affected by the tortuosity of the channels, which was affected by the pore structure and distribution of the particles. With the same porosity, and less tortuous channels, there was less resistance to gas flow produced by the channels. Therefore, the desorption efficiency was affected by the porosity of the sorbent bed and the tortuosity of the channels.

For DVB particles, the particle shapes were more irregular than those of CAR particles, which resulted in a decreased influence of the particle size on tortuosity, and therefore, porosity dominated the overall desorption efficiency. For CAR particles, desorption efficiency was affected by both porosity and tortuosity. Since smaller particles can be more efficiently packed inside the needle, the overall porosity should decrease with the decrease of the particle size, resulting in a lower permeability. Therefore, for NTDs packed with DVB of smaller size, the smaller porosity allowed expanded gas flow through the sorbent bed for a longer period of time, which might have increased the efficiency of analytes delivery and consequently increased the desorption efficiency. Additionally, the smaller porosity of the NTDs packed with DVB of smaller size might

have allowed higher linear velocity of gas flow through the surface of the sorbent, and resulted in a more efficient desorption.

For CAR NTDs, the CAR particles were more spherical; small particle size might produce much more tortuous channels than large particles. Although the gas flow time was longer, or the linear gas flow rate was higher due to the smaller porosity of the smaller particles, the much higher tortuosity still significantly restricted the analytes delivery in the channels, which resulted in less efficient desorption of NTDs packed with smaller CAR particles. This might explain the increase of the carryover percentage with the decrease of particle size for CAR NTDs, and also explain the opposite trend of the desorption efficiency with the decrease of particle size for DVB NTDs.

In addition, the desorption efficiencies for different types of NTDs were investigated using the carrier gas assisted desorption method. It was noted that for DVB needles, no carryover was detected for VOCs, and thus two PAH compounds were used for this investigation. The results are shown in Figures 4-4 and 4-5. The results are in good accordance with the results obtained by thermal expansion desorption.

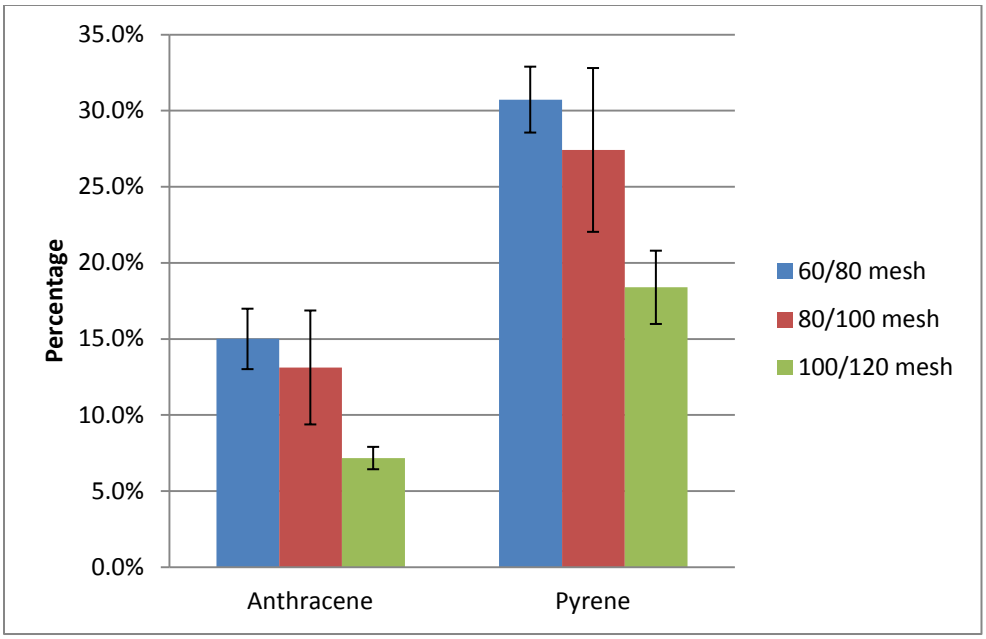


**Figure 4-4 Carryover percentages of NTDs packed with 1 cm DVB of different sizes with carrier gas assisted desorption (n=8: two needles, quadruplicate)**

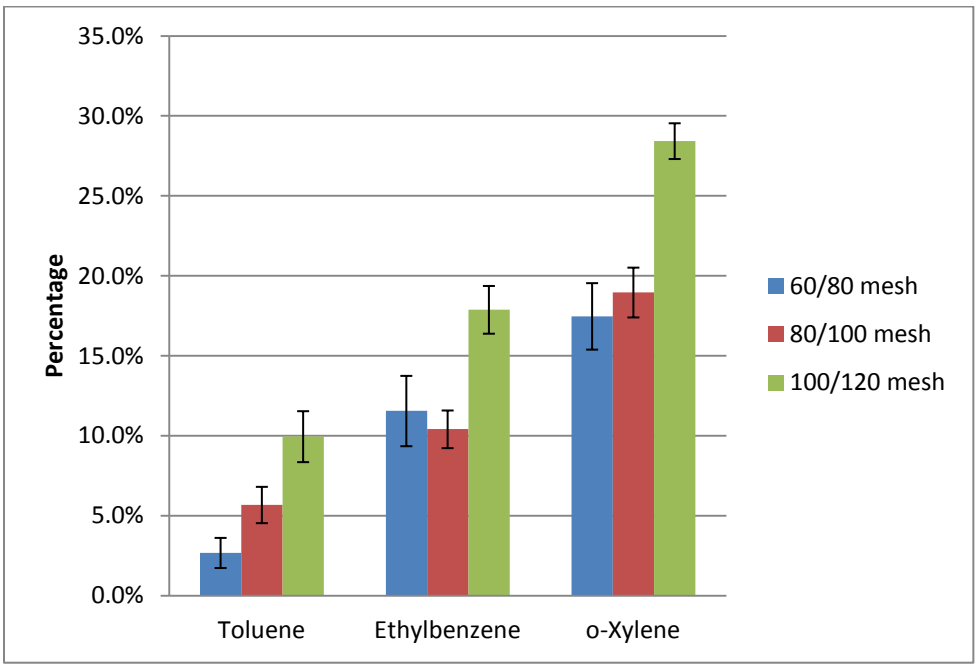


**Figure 4-5 Carryover percentages of NTDs packed with 1 cm CAR of different sizes with carrier gas assisted desorption (n=8: two needles, quadruplicate)**

### 4.3.3 Influence of external gas on desorption efficiency

External gas assisted desorption is a commonly used desorption method to improve the release of the analytes from the sorbent bed. Air, nitrogen, and helium are three commonly used gases. Due to the different viscosities of those gases, analytes present different diffusion coefficients in those gases, and therefore might display different mobilities passing through the channels of the sorbent bed. In this case, NTDs would show different desorption efficiencies with different assisting gases. To investigate the differences of the desorption efficiencies with different external gases, two NTDs packed with DVB of 60/80 mesh were used to extract 10 mL gaseous sample of pyrene and anthracene from a 20 mL vial and the first desorption was conducted for 0.3 min with 0.3 mL external gas. After the first desorption, NTDs were injected into the GC injector again for 2 min with 0.3 mL carrier gas to test the carryover. For NTDs packed with CAR of 60/80 mesh, two NTDs were used to extract 10 mL gaseous VOC sample from the gas standard generator. The first desorption was conducted for 0.5 min with 0.5 mL external gas, then the NTD was injected into the GC injector again with 0.5 mL helium for 2 min to test the carryover. The results are shown in Figure 4-6 and Figure 4-7.

As seen in Figures 4-6 and 4-7, the carryover percentages are almost the same with different external gases. Thus the external gas does not have a significant effect on the desorption efficiency for the compounds investigated. However, the use of air might increase the oxidation and decomposition of the adsorbent, which might shorten the sorbent life.

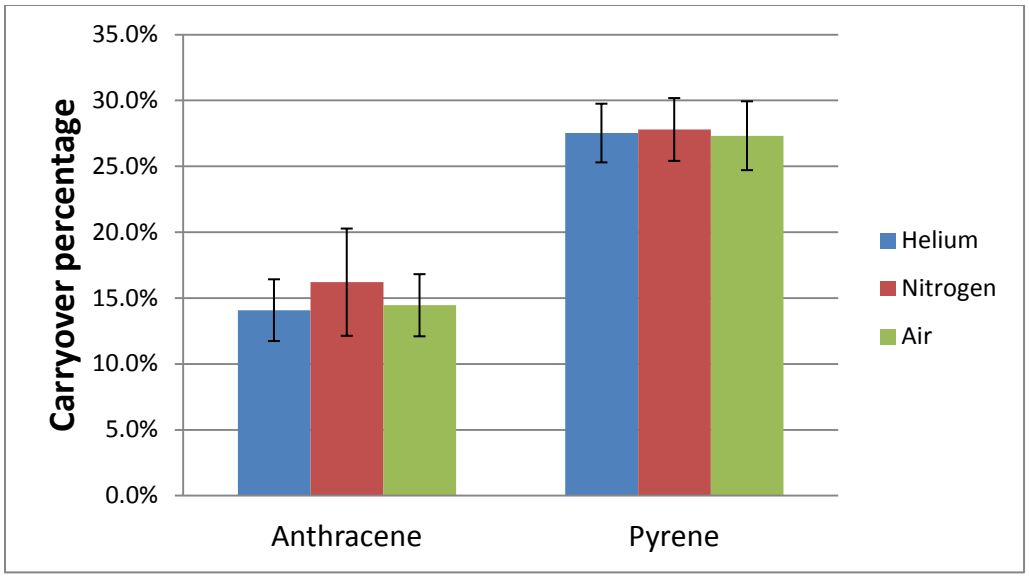


**Figure 4-6 Carryover percentages of DVB-NTDs with different external gas assisted desorption (n=8: two needles, quadruplicate)**

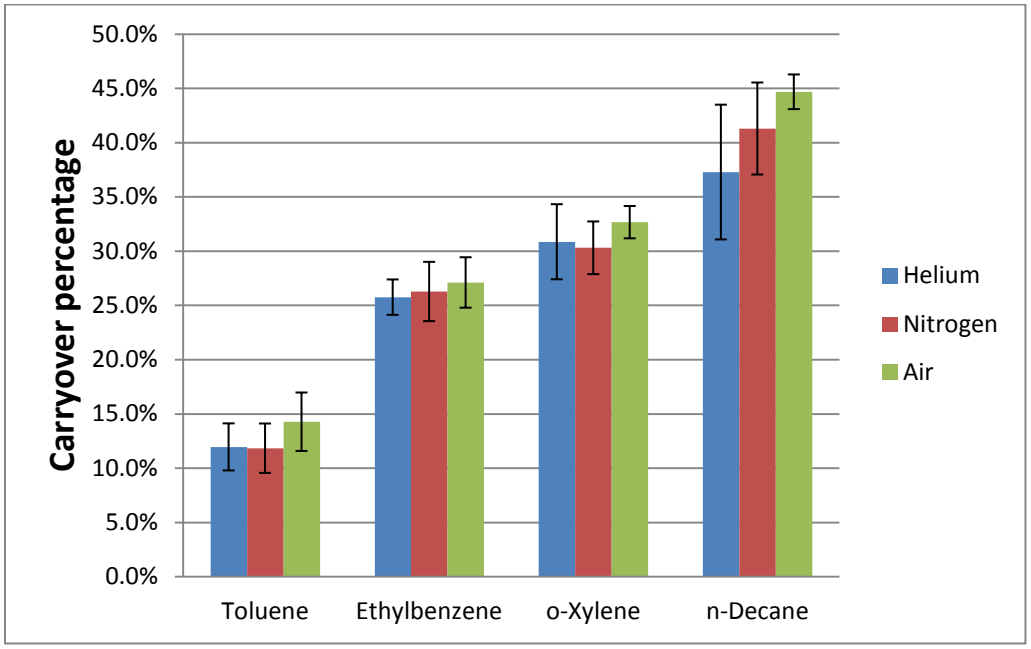


**Figure 4-7 Carryover percentages of CAR-NTDs with different carrier gas assisted desorption (n=8: two needles, quadruplicate)**

### 4.3.4 Influence of relative humidity on desorption efficiency

Improved desorption efficiency of the NTD was reported when a large amount of water vapour or droplets was presented inside the needle by packing alumina at the back of the sorbent to retain water vapour [36]. To investigate the influence of water vapour on the desorption efficiency of NTDs packed with sorbent only, two NTDs packed with 1 cm 60/80 mesh DVB and two NTDs packed with 1 cm 60/80 mesh CAR were used to sample TEX compounds at different relative humidities. The results are shown in Figures 4-8 and 4-9.

As shown in both figures, the desorption efficiency was not affected by the humidity level. This might be due to the poor retention of the water vapour by both adsorbents. Although the humidity level of the samples was different, the amount of water vapour extracted onto the adsorbents was similar, which resulted in similar desorption efficiencies. One solution to this might be to pack some adsorbent with strong water affinity at the back of the adsorbent to retain a large amount of water vapour. However, to generate 1 mL of water vapour during desorption, the NTDs have to retain around a 0.5 µL water droplet on the sorbent bed, which is really difficult in practice. While desorption could be easily improved by using 1 mL of external gas instead of retaining a large amount of water vapour on the sorbent regardless of the potential damage to the column by the water vapour, the water vapour assisted desorption method is not as widely accepted as the external gas desorption method due to the above limitations.

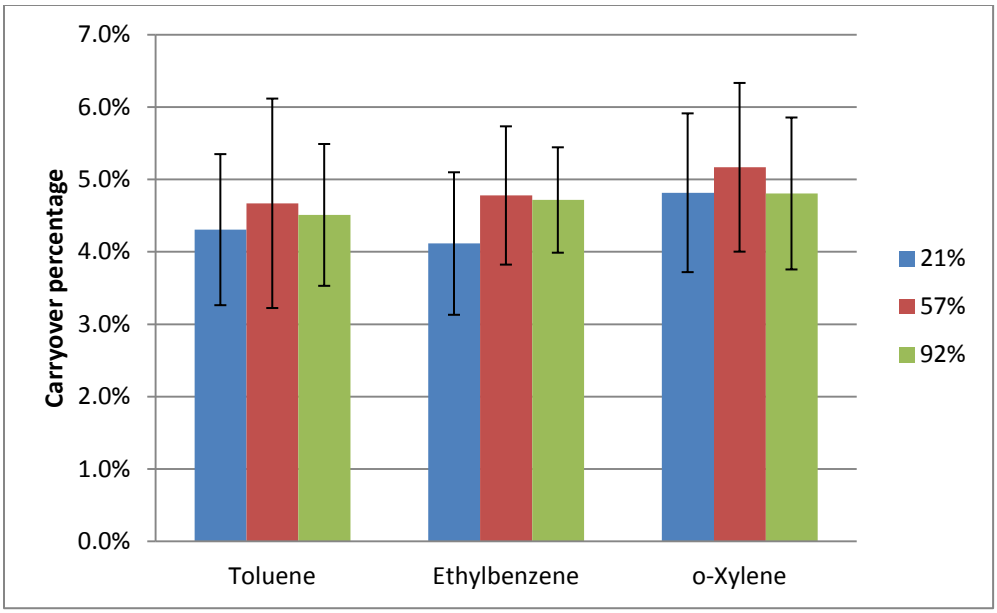


**Figure 4-8 Carryover percentages of DVB-NTDs with different humidities using thermal expansion desorption (n=8: two needles, quadruplicate)**

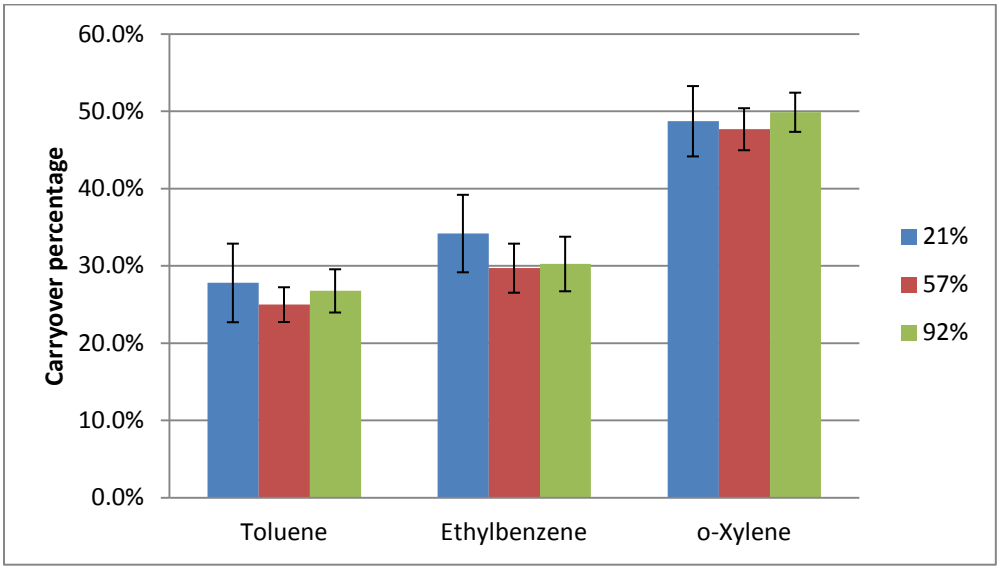


**Figure 4-9 Carryover percentages of CAR-NTDs with different humidities using thermal expansion desorption (n=8: two needles, quadruplicate)**

## 4.4 Conclusion

The desorption efficiencies of NTDs packed with DVB or CAR of different sizes were investigated using different desorption methods. It was found that the best desorption efficiency was obtained by the smallest particles for DVB and the largest particles for CAR, which is likely due to different pore structures and different tortuosity of the channels on the sorbent bed for the two adsorbents. The external gas assisted desorption method showed better desorption efficiency over thermal expansion desorption and water vapour assisted desorption. However, even with the external gas assisted desorption method, the carryover percentages of the CAR needles for the most volatile compounds were still significant. One good solution could be the introduction of carrier gas into the sorbent bed, having the gas flow through the sorbent bed to assist the desorption, by using a side hole needle (Figure 1-2-D) in combination with a narrow neck liner (Figure 1-3-B), which has already been demonstrated [17].

# Chapter 5 Particle sampling

## 5.1 Introduction

Theoretically, NTD can act as a filter and aerosol particles can be collected on the sorbent in the needle by passing aerosol samples through the device. A common misconception is that aerosol filters work like microscopic sieves in which only particles smaller than the holes can get through. This view may be appropriate for the liquid filtration of solid particles, but it is not how aerosol filtration works. As described in Chapter 1, particulates are removed by a filter by colliding with and attaching to the surface of the sorbent. The ability of the NTD to collect particles, characterized by the collection efficiency, is strongly related to the packing density, the sorbent particle size, the length of sorbent bed, the linear flow rate, as well as the diffusion constant and Stokes number of a particulate in aerosol. The objective of this work is to investigate the trapping efficiency of the NTDs for aerosol samples, and optimize trapping efficiency by optimizing the needle design and the trapping conditions. A simplified equation for the diffusion-controlled collection, which was proposed and validated in Otani's research using granular filters [49] and later applied to Li's work related to the NTD [44], will be used as the guidance for this work, where

$$E = 1 - \exp\left(\frac{-32\alpha L}{\pi d_p^{5/3} D^{2/3} u^{2/3}} + \frac{-64\alpha L d_s^2}{\pi d_p^3}\right) \qquad \text{for } Re < 30 \qquad (21)$$

In the equation, $D$ is the particle diffusion coefficient, $u$ is the superficial gas velocity, $Re$ is the Reynolds number, $d_p$ is the sorbent particle size, and $d_s$ is the sample particle size.

## 5.2 Experimental section

### 5.2.1 Chemicals and materials

Methanol and other solvents (HPLC grade) used in the experiments were obtained from Fisher Scientific (Ottawa, ON, Canada). $\alpha$-Pinene and 60/80 mesh CAR particles (surface area: 1200 $m^2/g$) were purchased from Sigma-Aldrich (Bellefonte, PA, USA). 60/80 mesh Tenax GC adsorbent was purchased from Chromatographic Specialties Inc. (Brockville, ON, Canada). DVB particles (surface area: 582 $m^2/g$) of 60/80 mesh, 80/100 mesh, and 100/120 mesh were purchased from Ohio Valley (Marietta, OH, USA). The 60 mm long 22-gauge needles with a side hole (I.D. 0.41 mm, O.D. 0.71 mm) were purchased from SGE Analytical Science (Australia). The ADM 1000 flow meter was purchased from Agilent Technologies (Mississauga, ON, Canada). A sampling pump with a mass controller and flow controller was purchased from PAS (Germany). Extra dry compressed air was supplied by Praxair Canada Inc. (Kitchener, ON, Canada).

### 5.2.2 Aerosol generator and gas standard generator

An 800 mL NaCl solution (0.1 g/L) spiked with α-pinene solution (20 µL in 5 mL methanol) was prepared in the storage bottle as the matrix. A constant output atomizer (model 3076, TSI Inc., Shoreview, MN, US) was used to generate polydisperse aerosol particles, from 10 nm to 200 nm, with a median around 100 nm, at a concentration around $2\times10^6$ particles/ mL, as shown in Figure 5-1.

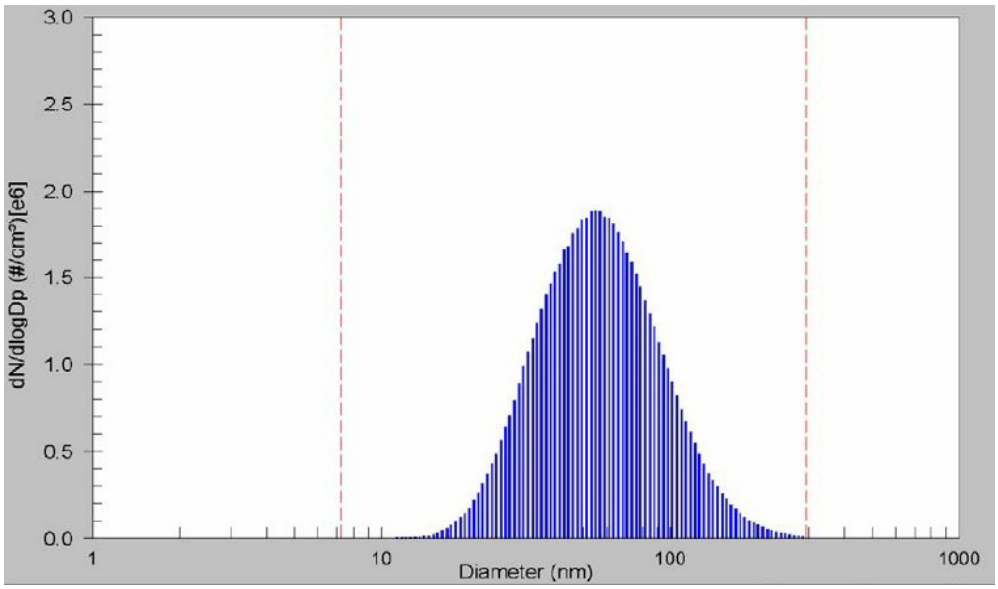


**Figure 5-1 Particle size and distribution of a sodium chloride aerosol generated from 0.1 mg/cm$^2$ solution [50]**

### 5.2.3 Needle trap preparation

To prepare the NTD, a stainless spring plug was fixed and pressed into the tip of a needle. Then, sorbent particles were aspirated into the needle by a tap-water aspirator and held by the spring plug. After packing the desired length of sorbent bed, another spring plug was pressed onto the sorbent bed. Then each needle was conditioned in the hot GC injector installed with a narrow-neck metal liner for 1 hour. The conditioning temperature was 250 °C for DVB needles, and 300 °C for both CAR and Tenax needles. The schematic diagram of the needle used is illustrated in Figure 5-2.

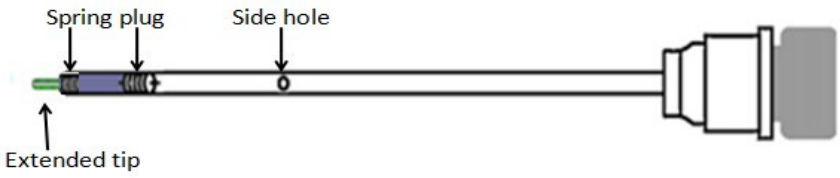


**Figure 5-2 Schematic diagram of a packed needle**

### 5.2.4 Sampling and desorption

Two NTDs were connected in sequence, with the back NTD connected to the sampling pump. Then 50 mL of aerosol sample was pumped through the NTDs at certain flow rates. Because of early breakthrough of NTDs packed with Tenax GC, only 10 mL of aerosol sample was collected for those needles. After sampling, the NTDs were removed from the pump and separately injected into a GC injector for 1 min. The injector temperature was 250 °C for DVB needles, and 300 °C for both CAR and Tenax needles. The desorption efficiency was determined using the following relationship:

$$E = \frac{The\ amount\ of\ the\ analyte\ on\ the\ first\ needle}{The\ amount\ of\ the\ analyte\ on\ the\ first\ and\ the\ second\ needle} \quad (22)$$

### 5.2.5 Instrumentation

A Varian CP-3800 gas chromatograph/flame ionization detector (GC/FID), fitted with a DB-5HS column (30 m × 0.25 mm × 0.25 μm) (J&W Scientific, Mississauga, ON, Canada) was used to separate and analyze the target compounds. The injector temperature was 250 °C for DVB needles, and 300 °C for CAR needles. The injection was made in splitless mode with a narrow-neck liner from SGE. The initial oven temperature was set at 50 °C and held for 1 min, then ramped up to 150 °C at a rate of 25 °C/min, and held at 150 °C for 1 min.

## 5.3 Results and discussion

### 5.3.1 Selection of sorbent

A theoretical calculation based on single sorbent theory has already been described in Chapter 1, and indicates that the sorbent particle size inside the needle is the

most important factor affecting the total collection efficiency of an NTD. Since the sorbent packed inside an NTD contains porous particles rather than solid beads, the collection efficiency will be affected significantly by both the sorbent particle size, and intra- and inter-particle pore size and distribution. To investigate the influence of intra- and inter-particle pore size and distribution on the collection efficiency, NTDs packed with different adsorbent particles (CAR, DVB, and Tenax) of 60/80 mesh were used for particle sampling, and the result is presented in Figure 5-3.

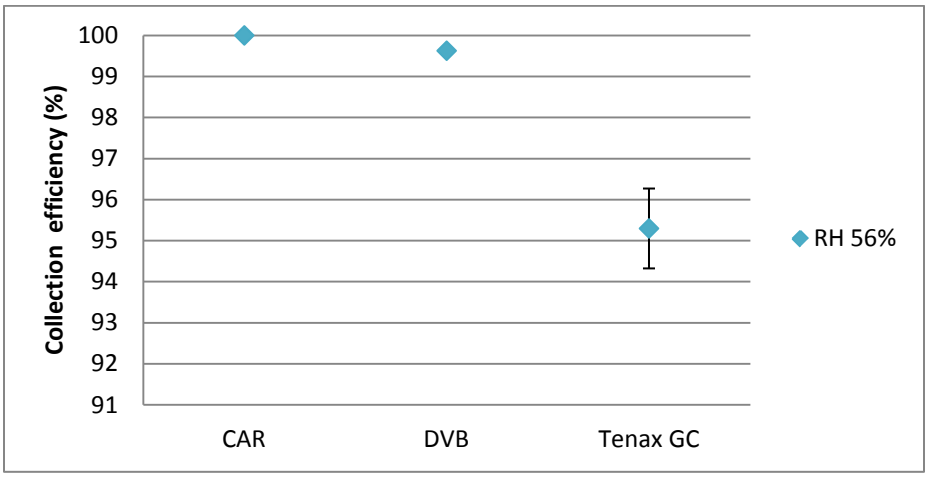


**Figure 5-3Collection efficiencies of NTDs packed with different sorbent particles of 60/80 mesh (n=4: two needles, duplicate for each needle.)**

As shown in Figure 5-3, the CAR needles presented the highest collection efficiency for the aerosol sample, while the Tenax needles displayed around 5% penetration, probably due to different pore sizes and distributions. It should be noted though that it is extremely difficult to know the intra- and inter-particle size and distribution in practice. One simple solution is to estimate the average pore size by calculating the hydrodynamic diameter of the sorbent bed, based on the assumption that the sorbent bed is made of spherical beads that attach to each other. Given that the

average pore size is equal to the hydrodynamic diameter, the average pore size is calculated to be 0.01 μm for CAR needles, 0.03 μm for DVB needles, and 0.58 μm for Tenax GC needles by using the equation that $d_H = \frac{6V}{S_e}$, where $d_H$ is the hydrodynamic diameter, $V$ is the total volume of the sorbent particle, and $S_e$ is the total surface area of the particles inside the needle. It is noted that collection efficiency decreases with the increase of average pore size of the sorbent bed. It should also be noted that all of the NTDs have high collection efficiency (above 95%) for the particulate size range investigated, but theoretically calculated collection efficiency based on Equation (16) is 4% for CAR needles, 6% for DVB needles, and 5% for Tenax GC needles, by assuming that those particles are spherical solid beads. Such a difference could be attributed to the pores inside each sorbent particle, which might act as micro filters and play a significant role in the particle trapping. It should be noted that the aerosol sample investigated contained around 15% free molecules and around 85% particulate-bound molecules according to a previous study [44], in which case penetration was not necessarily caused by the penetration of the particulates. To verify that penetration was only caused by the penetration of the particulates, the same devices were utilized to sample gaseous $\alpha$-pinene from the gas standard generator with a concentration about equal to the total concentration of the aerosol sample. No penetration was found for either DVB or Tenax needles under the same experimental conditions, indicating that the penetration only resulted from the penetration of the particulates.

### 5.3.2 Influence of solidity on collection efficiency

As shown in Equation (21), the increase in solidity α will increase the collection efficiency. The solidity of a sorbent bed could be increased by more efficient packing. Sorbent particles with smaller size tend to pack more efficiently than larger sized particles. Thus, for the same adsorbent, NTDs packed with smaller particles should exhibit higher collection efficiency. To verify this, three types of NTDs were packed with 1 cm DVB of 60/80 mesh, 80/100 mesh, and 100/120 mesh, respectively, at a solidity of 0.32, 0.37, and 0.40. Then, those NTDs were used for particle sampling, and the results are shown in Figure 5-4. As shown in Figure 5-4, the collection efficiency does not change with a decrease in solidity.

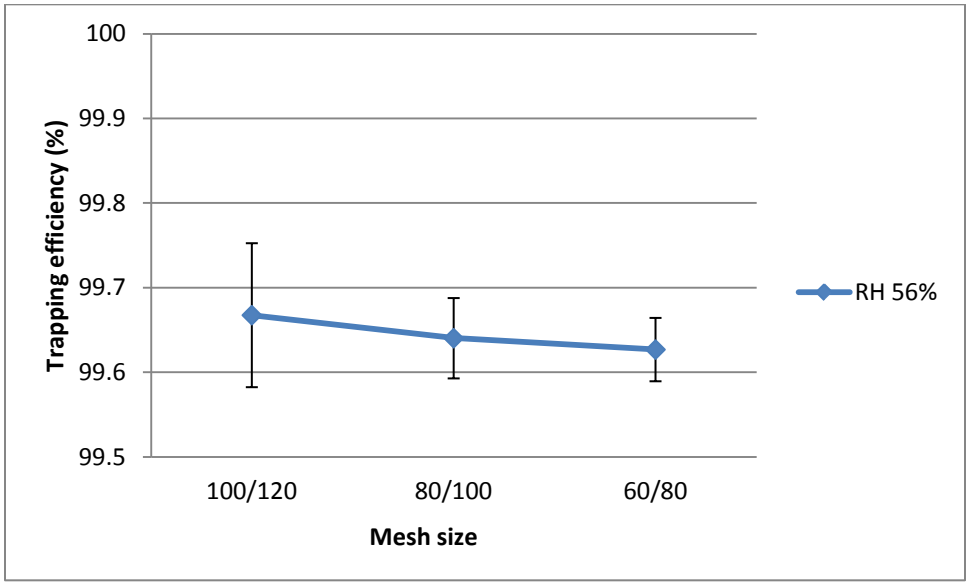


**Figure 5-4 Collection efficiencies of NTDs packed with DVB of 60/80 mesh, 80/100 mesh and 100/120 mesh (n=4: two needles, duplicate for each needle.)**

### 5.3.3 The influence of sampling flow rate and relative humidity on collection efficiency

The effect of the sampling rate and the relative humidity on the collection efficiency was also studied, as shown in Figure 5-5. The collection efficiency decreased with the increase in sampling rate at high humidity level. It is quite intuitive that the increase in sampling rate results in an increase in facial velocity, and consequently results in a decrease of the collection efficiency, as indicated in Equation (21). However, the collection efficiency only decreased slightly with a significant increase in sampling rate. This is very important since, in practice, to save sampling time, a faster sampling rate is usually desired for the compensation of slightly lower collection efficiency. At lower humid level, the collection efficiency did not exhibit any changes which might probably due to the difference in sampling rate was not big enough to cause a change in collection efficiency.

It should be noted that higher humidity would improve the collection efficiency with different sampling rates. This might be due to the fact that at different humidity levels, aerosol particles display different dynamic diameters, which impacts their ability to be collected.

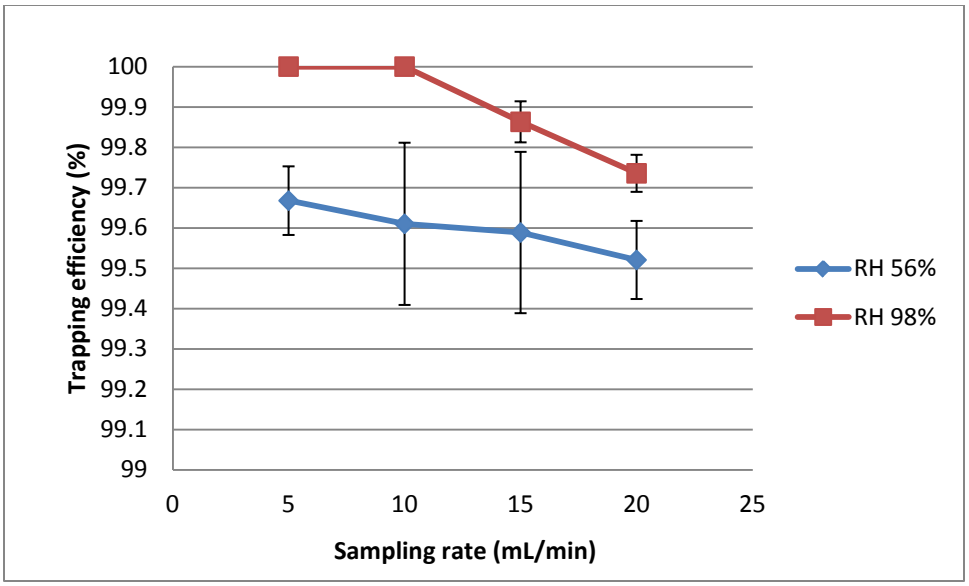


**Figure 5-5 Collection efficiencies of NTDs packed with 100/120 mesh DVB under different sampling rates and different humidity levels (n=6: two needles, triplicate for each needle.)**

### 5.3.4 Reusability

Theoretically, for particulate sampling, each needle can be used only once, because after the sampling, solid particles will be retained on the sorbent bed, which might change the performance of the needle. However, in practice, each needle could be used as many times as possible until the occurrence of significant changes (e.g. 5%) of the fundamental parameters, such as the permeability, the capacity, and the desorption efficiency. A preliminary investigation has already been done in Warren's work [17] showing that for on-site application, each needle could be used up to 5 times without changing the capacity. This was confirmed in the experiment where most needles were used up to 5 times without significantly changing the permeability and extraction amount. The reusability might greatly reduce the cost of an NTD for on-site application for aerosol sampling, making NTD a potential alternative of membrane filters.

## 5.4 Conclusion

The collection efficiency of the NTDs packed with different sorbent particles was investigated with the guidance of the single filter theory. It was found that the pore size and distribution, which is determined by the sorbent particle size and porosity, and characterized by average pore size and estimated by hydrodynamic diameter, had a dominant influence on the collection efficiency. The collection efficiency increased with a decrease in the hydrodynamic diameter of the sorbent bed. The collection efficiency also increased with an increase in the solidity of the sorbent bed, the humidity of the aerosol sample, and a decrease in sampling flow rate. Such trends are in good agreement with the theory. It was also noted that almost all of the NTDs used presented extremely high collection efficiency for aerosols around 0.1 μm, indicating a great potential of the NTD as a filter for aerosol collection. With the presence of free molecules in the aerosol sample, NTD will be able to act as both an adsorbent and a filter to trap both free molecules and particulates to determine the total concentration of the analytes in the sample.

Future studies will focus on investigating the collection efficiency of the NTD with the optimized packing for particles from 10 nm to 10 μm, and utilizing the NTD for on-site applications.

# Chapter 6 Conclusion and future studies

The fundamental parameters of the NTD were investigated with respect to different packing materials and particle dimensions, and the proposed theory was validated. It was found that smaller particles could be more densely packed, which resulted in a higher capacity but also higher resistance; the resistance increased much faster than the capacity. Comparing the capacity and permeability of NTDs packed with particles of different sizes, it would be preferable to pack the NTD with a longer sorbent bed using larger particles (i.e. 2 cm 60/80 mesh DVB), rather than packing the NTD with a shorter sorbent bed using smaller particles (i.e. 1 cm 100/120 mesh DVB), especially for active sampling.

The desorption efficiency of an NTD was mainly affected by the permeability of the sorbent bed and probably the tortuosity of the channels. Thus, higher permeability did not necessarily result in better desorption efficiency. For DVB needles, the desorption efficiency increased with the decrease of the sorbent particle size, while for CAR needles, the desorption efficiency decreased with the decrease of the sorbent particle size. Taking the capacity into account, for NTDs packed with single adsorbent, it would be preferable to use 100/120 mesh DVB or 60/80 mesh CAR for the analysis of a narrow range of target compounds. However, when segmented sorbents are used, it is still preferable to utilize larger sorbent particles to get higher permeability, since a high permeability is the priority to get effective extraction and desorption.

Also shown in the results, an external gas-assisted desorption method was more effective than a thermal expansion desorption approach, but this method still presented

significant carryover for extremely strong adsorbents such as CAR. To get better desorption efficiency for the NTDs packed with extremely strong adsorbent, the carrier gas flow approach, utilizing a side hole needle in combination with a narrow-neck liner, should be a better option.

For particulate sampling, it was found that NTDs packed with different particles presented high collection efficiency for the particles investigated, and the collection efficiency was probably determined by the pore size and distribution of the sorbent bed packed inside the needle. The collection efficiency increased with an increase in humidity of the aerosol sample, and a decrease in the sampling rate. Future work should focus on investigating the particle collection efficiency of needle traps for particles over a wider size range, from 10 nm to 10 microns. Another interesting area would be the development of NTDs for on-site applications to determine the total concentration of free and particle-bound analytes in the environment. With a combination of SPME fibre for the determination of the free concentration of analytes, the free vs. total concentrations can be determined.

## References


[1] J. Pawliszyn, Handbook of Solid Phase Microextraction, Chemical Industry Press, Beijing, 2009.

[2] A. Sarafraz-Yazdi, A. Amiri, Trends Anal. Chem. 29 (2010) 1-14.

[3] M. Ras, F. Borrull, R. Marce, Trends Anal. Chem. 28 (2009) 347-361.

[4] C. Nerin, J. Salafranca, M. Aznar, R. Batlle, Anal. Bioanal. Chem. 393 (2009) 809-833.

[5] H. Lord, W. Zhan, J. Pawliszyn, Anal. Chim. Acta 677 (2010) 3-18.

[6] A. Lewis, K. Bartle, J. McQuaid, M. Pilling, P. Seakins, J. High Resol. Chromatogr. 19 (1996) 686-690.

[7] J. Wang, S. Chen, C. Chew, J. Chromatogr. A 863 (1999) 183-193.

[8] J. Wang, W. Chen, Y. Lin, C. Tsai, J. Chromatogr.A 896 (2000) 31-39.

[9] A. Keil, H. Hernandez-Soto, R. Noll, M. Fico, L. Gao, Z. Ouyang, R. Cooks, Anal. Chem. 80 (2008) 734-741.

[10] A. Mastrogiacomo, E. Pierini, L. Sampaolo, Chromatographia 52 (2000) 345-350.

[11] K. Demeestere, J. Dewulf, B. Witte, H. Langenhove, J. Chromatogr. A 1153 (2007) 130-144.

[12] F. Raschdorf, Chimia 32 (1978) 478-483.

[13] T. Qin, X. Xu, T. Polak, V. Pacakova, K. Stulik, L. Jech, Talanta 44 (1997) 1683-1690.

[14] J. Koziel, M. Odziemkowski, J. Pawliszyn, Anal. Chem. 73 (2001) 47-54.

[15] A. Wang, F. Fang, J. Pawliszyn, J. Chromatogr. A 1072 (2005) 127-135.

[16] I. Eom, J. Pawliszyn, J. Sep. Sci. 31 (2008) 2283-2287.

[17] J. Warren, Needle Trap Device and Solid Phase Microextraction Combined with Portable GC-MS for On-Site Applications, Master thesis, University of Waterloo, 2011. (url:http://hdl.handle.net/10012/6014)

[18] M. Jochmann, X. Yuan, B. Schilling, T. Schmidt, J. Chromatogr. A 1179 (2008) 96-105.

[19] Z. Altun, M. Abdel-Rehim, L. Blomberg, J. Chromatogr. B 813 (2004) 129-135.

[20] Y. Saito, I. Ueta, K. Kotera, M. Ogawa, H. Wada, K. Jinno, J. Chromatogr. A 1106 (2006) 190-195.

[21] Y. Saito, I. Ueta, M. Ogawa, K. Jinno, Anal. Bioanal. Chem. 386 (2006) 725-732.

[22] I. Ueta, Y. Saito, M. Hosoe, M. Okamoto, H. Ohkita, S. Shirai, H. Tamura, K. Jinno, J. Chromatogr. B 877 (2009) 2551-2556.

[23] M. Ogawa, Y. Saito, S. Shirai, Y. Kiso, K. Jinno, Chromatographia 69 (2009) 685-690.

[24] M. Ogawa, Y. Saito, I. Ueta, K. Jinno, Anal. Bioanal. Chem. 388 (2009), 619-625.

[25] Y. Saito, I. Ueta, M. Ogawa, M. Hayashida, K. Jinno, J. Pharm. Biomed. Anal. 44 (2007) 1-7.

[26] Y. Gong, I. Eom, D. Lou, D. Hein, J. Pawliszyn, Anal. Chem. 80 (2008) 7275-7282.

[27] R. Kubinec, V. Berezkin, R. Gorova, G. Addova, H. Mracnova, L. Sojak, J. Chromatogr. B 800 (2004) 295-301.

[28] I. Eom, V. Niri, J. Pawliszyn, J. Chromatogr. A 1196-1197 (2008) 10-14.

[29] H. Jurdakova, R. Kubinec, M. Jurcisinova, Z. Krkosova, J. Blasko, I. Ostrovsky, L. Sojak, V. Berezkin, J. Chromatogr. A 1194 (2008) 161-164.

[30] J. Sanchez, R. Sacks, Anal. Chem. 75 (2003) 2231-2236.

[31] M. Mieth, S. Kischkel, J. Schubert, D. Hein, W. Miekisch, Anal. Chem. 81 (2009) 5851-5857.

[32] D. Lou, X. Lee, J. Pawliszyn, J. Chromatogr. A 1201 (2008) 228-234.

[33] Y. Saito, I. Ueta, M. Ogawa, A. Abe, K. Yogo, S. Shirai, K. Jinno, Anal. Bioanal. Chem. 393 (2009) 861-869.

[34] H. Bagheri, Z. Ayazi, A. Aghakhani, Anal. Chim. Acta, 683 (2011) 212-220.

[35] O. Sae-Khow, S. Mitra, J. Chromatogr. A 1216 (2009) 2270-2274.

[36] P. Prikryl, R. Kubinec, H. Jurdakova, J. Sevcik, I. Ostrovsky, L. Sojak, V. Berezkin, Chromatographia 64 (2006) 65-70.

[37] V. Berezkin, E. Makarov, B. Stolyarov, J. Chromatogr. A 985 (2003) 63-65.

[38] V. H. Niri, I. Eom, F. R. Kermani, J. Pawliszyn, J. Sep. Sci. 32 (2009) 1075-1080.

[39] M. Harper, Ann. Occup. Hyg. 37 (1993) 65-88.

[40] F. Cropper, S. Kamlnsky, Anal. Chem. 35 (1963) 735-743.

[41] G. Senum, Environ. Sci. Technol. 15 (1981) 1073-1075.

[42] P. Lovkvist, J. Jonsson, Anal. Chem. 59 (1987) 818-821.

[43] F.A.L. Dullien, Porous Media, Academic Press, Inc., San Diego, 1992.

[44] X. Li, G. Ouyang, H. Lord, J. Pawliszyn, Anal. Chem. 82 (2010) 9521-9527.

[45] W.C. Hinds, Aerosol Technology: Properties, Behavior, and Measurement of Airborne Particles, 1st ed., John Wiley & Sons, Inc., New York, 1982.

[46] K. Lee, B. Liu, Aerosol Sci. Technol. 1 (1982) 147-161.

[47] M. Matyka, A. Khalili, Z. Koza, Phys. Rev. E 78 (2008) 026306.

[48] M. Mieth, J. Schubert, T. Groger, B. Sabel, S. Kischkel, P. Fuchs, D. Hein, R.

Zimmermann, W. Miekisch, Anal. Chem. 82 (2011) 2541-2551.

[49] Y. Otani, C. Kanaoka, H. Emi, Aerosol Sci. Technol. 10 (1989) 463-474.

[50] Operation and Service Manual, Model 3076 Constant Atomizer, TSI Inc., 2008